

The role of motor cortex in motor sequence execution depends on demands for flexibility

Received: 18 July 2023

Accepted: 18 September 2024

Published online: 4 November 2024

 Check for updates

Kevin G. C. Mizes^{1,2}✉, Jack Lindsey³, G. Sean Escola⁴✉ & Bence P. Ölveczky^{1,2}✉

The role of the motor cortex in executing motor sequences is widely debated, with studies supporting disparate views. Here we probe the degree to which the motor cortex's engagement depends on task demands, specifically whether its role differs for highly practiced, or 'automatic', sequences versus flexible sequences informed by external cues. To test this, we trained rats to generate three-element motor sequences either by overtraining them on a single sequence or by having them follow instructive visual cues. Lesioning motor cortex showed that it is necessary for flexible cue-driven motor sequences but dispensable for single automatic behaviors trained in isolation. However, when an automatic motor sequence was practiced alongside the flexible task, it became motor cortex dependent, suggesting that an automatic motor sequence fails to consolidate subcortically when the same sequence is produced also in a flexible context. A simple neural network model recapitulated these results and offered a circuit-level explanation. Our results critically delineate the role of the motor cortex in motor sequence execution, describing the conditions under which it is engaged and the functions it fulfills, thus reconciling seemingly conflicting views about motor cortex's role in motor sequence generation.

While motor cortex (MC) is generally thought of as the main controller of voluntary movements in mammals^{1–4}, its supremacy is challenged by near-complete recoveries of many behaviors following MC lesions^{5–11}. The most consistent control deficit following such lesions is the inability to generate individuated movements of distal joints and digits, a level of dexterity uniquely afforded by MC's projections to the spinal cord^{5,11,12}. It's also been suggested that MC modulates movements generated by lower motor centers in response to unexpected perturbations, such as avoiding obstacles during locomotion^{9,13,14}. However, it likely does more than just enable dexterous or corrective movements. MC sits atop the mammalian motor hierarchy with access to all parts of the subcortical control infrastructure^{13,15} and, hence, is well situated to affect motor output beyond the direct and continuous control of muscles^{9,14,16–19}. For example, motor cortical projections to the striatum are essential for learning some motor skills that, once acquired, can be generated subcortically, suggesting a role for MC in learning that

is independent of its role in control^{20,21}. Given MC's projections to subcortical motor circuits, it could also orchestrate sequences comprising basic movements and actions^{6,7,22,23} that, when executed in isolation, can be fully specified and controlled by subcortical circuits.

While many stereotyped motor sequences, both learned and innate, can be controlled subcortically^{6,13,24–28}, we hypothesize that motor sequences assembled in response to instructive cues require MC even if the execution of the individual elements in the sequence does not. The idea is that MC funnels relevant information parsed by distributed cortical circuits (for example, about environmental events, memory processes and learned rules and associations) to subcortical motor centers, thus allowing them to be used in flexible and adaptive ways^{9,29} (Fig. 1a). We argue that rats are uniquely suited for probing this idea for two main reasons. First, their reliance on MC for the control of basic movements and actions—and even some stereotyped learned motor sequences assembled from these—is modest compared with

¹Program in Biophysics, Harvard University, Cambridge, MA, USA. ²Department of Organismic and Evolutionary Biology and Center for Brain Science, Harvard University, Cambridge, MA, USA. ³Zuckerman Mind Brain and Behavior Institute, Columbia University, New York City, NY, USA. ⁴Department of Psychiatry, Columbia University, New York City, NY, USA. ✉e-mail: kmizes@g.harvard.edu; sean.escola@gmail.com; olveczky@fas.harvard.edu

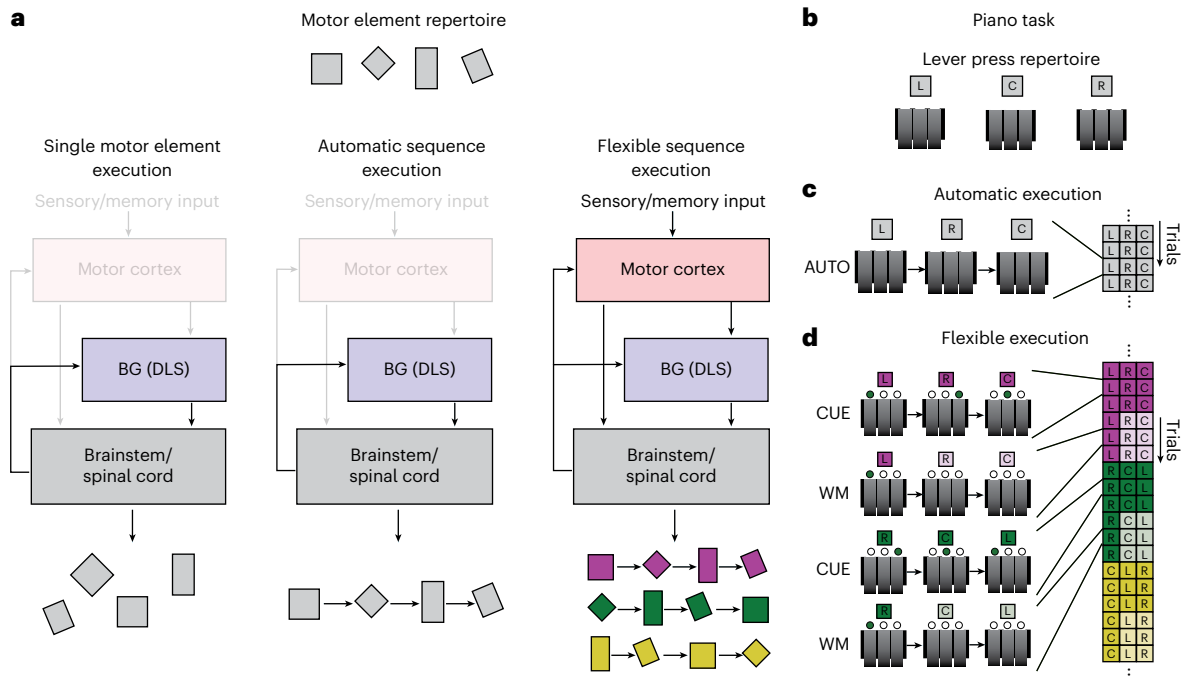


Fig. 1 | Addressing the role of motor cortex in the execution of automatic and flexible motor sequences. **a**, Simplified schematic representation of the motor control system considered in this study, and our hypotheses about how it is used in response to different challenges. Subcortical controllers can generate a wide range of species-typical motor elements (left) and highly practiced, that is, ‘automatic’, motor sequences assembled from these (center) without MC. However, we posit that ordering the same motor elements into different sequences informed by sensory inputs or WM (that is, ‘flexible’ motor sequences) depends on MC (right). **b**, ‘Piano-task’ paradigm to probe the role of MC in

generating automatic and flexible motor sequences. Rats are rewarded for performing a prescribed three-element sequence of lever presses on each trial. **c**, In the AUTO task, the same sequence is rewarded for the duration of the experiment. **d**, In the ‘flexible’ task, a different sequence is rewarded on a given block of six trials. The prescribed sequence in a block is randomly chosen and signaled by visual cues for the first three trials (CUE condition) and then by remembering the sequence for the remaining three trials (WM condition; Methods).

humans and nonhuman primates, as evidenced by even large lesions preserving such behaviors^{6,7,9,10,12}. Thus, by designing tasks for rats around species-typical movements that can be generated by subcortical motor regions^{6,10,20}, we can probe the necessity of MC in different task conditions without the ambiguity of it also being required for basic movement control.

Second, rats can master discrete sequence production tasks³⁰ akin to those frequently used in human and nonhuman primate studies of motor sequence learning and execution^{22,31,32}. The rich structure of such tasks allows us to probe MC’s necessary role in the flexible sequencing of basic movements and actions. Furthermore, by separately training rats to produce a single overtrained motor sequence to the point of automaticity³⁰, we can directly compare and contrast the relative contributions of MC to flexible versus automatic motor sequences. In the present study, we use the term ‘automatic’ to refer to the distinct qualities associated with single overtrained sequences, which we and others have found to be—on average—significantly faster, smoother and less error-prone than the same sequences executed in response to cues^{33,34}. We contrast these with ‘flexible’ motor sequences, which we define here as sequences of actions assembled on the fly in response to learned sensorimotor associations, much like the pianist playing a sonata from sheet music.

Using a discrete sequence production^{22,31,32} task adapted for rats (the ‘piano’ task), in combination with targeted lesions and neural network modeling, we show that the execution of a single overtrained, or automatic, motor sequence of lever presses and orienting movements is resilient to MC lesions^{6,21}. In contrast, we find that MC is necessary for generating similar sequences of lever presses when assembled in response to sensory cues or guided by working memory (WM). This stark dichotomy suggests that MC’s role in motor sequence generation

depends on the high-level demands of the task in a way that is independent of the specific motoric challenges. Intriguingly, automatic motor sequences, which were resilient to MC lesions when trained in isolation, became sensitive to lesions when practiced alongside the cortically dependent cue-guided task, suggesting that the flexible reuse of motor elements interferes with the subcortical consolidation of automatic motor sequences. Our network model offered a circuit-level explanation for these findings—subcortical consolidation of frequently used motor sequences relies on future sequence elements being consistently predictable from current and past ones. While this is the case for highly stereotyped single motor sequences, the unambiguous link between past and future behavior is broken when the elements of an overtrained sequence are also expressed in a flexible context, thus preventing subcortical consolidation.

Results

Motor cortex is dispensable for executing single automatic motor sequences

To delineate MC’s role in motor sequence execution, we used our previously developed three-lever ‘piano task’³⁰, in which rats are rewarded for performing sequences of three lever presses in a prescribed order (Fig. 1b–d). By varying how a rewarded sequence is specified, we can test whether and how MC’s role differs as a function of different task demands^{31,35}. In the ‘automatic’ (AUTO) task, animals are trained to execute the same single sequence until it is automatic; in the ‘flexible’ task, instructive visual cues (CUE condition)—or the memory of recently executed sequences informed by such cues (WM condition)—specify the rewarded sequence (Methods). Having previously found that stereotyped learned motor skills acquired in a timed lever-pressing task can be consolidated subcortically and executed without MC⁶,

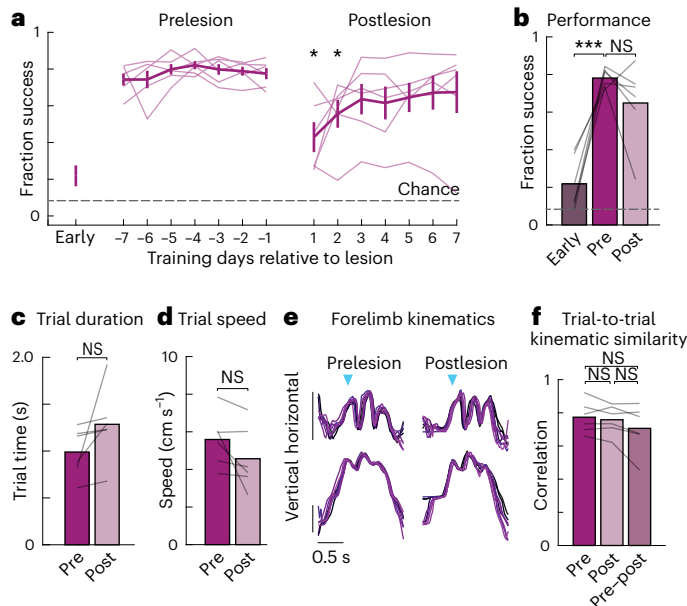


Fig. 2 | Automatic motor sequence execution is robust to motor cortex lesion. **a**, Performance on the automatic task, in which the same sequence of three lever presses is rewarded throughout. Data from the first week of training (early), the week before bilateral MC lesions (prelesion) and the first week of training after recovery (postlesion), averaged over the population ($n = 6$, error bars are s.e.m.). Lines denote individual rats. Stars denote whether performance on a given day is significantly different from average prelesion performance. **b**, Average performance of rats ($n = 6$) in the first week of training (early), the week before (pre) and days 3–7 following (post) MC lesion, accounting for surgery-related recovery. Lines denote individual rats. Postlesion performance is significantly above chance levels ($P = 0.0014$, one-sampled two-sided t test, where chance is defined as performing a random three-lever sequence consisting of press and orient movements). **c**, Trial times averaged over 1,000 trials before and after bilateral lesions, for each rat ($n = 6$; Methods). **d**, As in **c** for trial speeds. **e**, The movement kinematics of the active forelimb on eight example trials with similar durations overlaid and compared before and after MC lesions in an example rat. Blue arrows indicate the time of the first lever press, and vertical bars indicate 100 pixels (Supplementary Videos 1–3) or approximately 3.5 cm. **f**, Similarity in forelimb movement trajectories, measured through the average trial-to-trial trajectory correlations of each rat ($n = 6$), calculated from trials before the lesion, after the lesion, and by comparing trials across the lesion conditions (Methods). Trajectories are local-linearly warped to the lever taps. * $P < 0.05$ and *** $P < 0.001$, two-sided paired t test. NS, not significant.

we wanted to probe whether that result generalizes to automatic motor sequences trained in the piano task or, alternatively, whether this task is qualitatively different in terms of its reliance on MC. In contrast to the timed lever-pressing task, which explicitly requires high temporal precision and is solved by learning and consolidating a task-specific continuous movement pattern, the piano task is solved by sequencing discrete orienting and forelimb movements without any requirements for temporal precision. While both tasks result in stereotyped and fluid task-specific movement patterns^{6,30}, their acquisitions are thought to involve distinct initial learning and control processes³². Furthermore, discrete movement sequences, in contrast to continuous motor skills, are often thought to be consolidated at the cognitive, not the motoric level^{32,35}. Thus, it is unclear to what degree results from one type of behavior generalize to the other. To probe this, we lesioned MC bilaterally in rats overtrained on a single three-lever sequence, targeting both M1 and M2 as in previous work⁶ ($n = 6$ rats; Fig. 2 and Extended Data Fig. 1; Methods).

Consistent with our previous results^{6,21}, we found that the stereotyped overtrained motor sequences in the automatic task (Fig. 1c)

were largely resilient to bilateral MC lesions (Fig. 2a,b and Supplementary Video 1). While we saw a transient drop in performance after the resumption of training postlesion, this was consistent with nonspecific effects of the surgery procedure and subsequent recovery^{6,21}, with all but one rat recovering to prelesion performance within the first few days. This ‘outlier’ rat had converged on an unusual motor strategy, using a highly contorted posture to access the levers, perhaps requiring more sophisticated or dexterous control functionality uniquely afforded by cortical motor circuits^{6,9,10} (Supplementary Video 2).

The detailed learned movement patterns associated with the task were also largely unaffected by MC lesions. Average trial times and trial speeds, established signatures of automaticity^{33,34}, did not change significantly after lesions (Fig. 2c,d), nor did the highly stereotyped and idiosyncratic forelimb kinematics associated with the learned sequence (Fig. 2e,f). These results suggest that the automatic motor sequence had been consolidated subcortically, a finding consistent with previous work^{6,20,26}.

Motor cortex is required for flexible motor sequences instructed by sensory cues or working memory

Having established that an overtrained automatic sequence of forelimb and body-orienting movements can be performed without MC, we next used the rich structure of our piano task to probe whether MC is required when the three-element motor sequences are assembled in response to learned cue-action associations (the ‘flexible’ task; Fig. 1d). To do this, we challenged a different cohort of rats ($n = 7$) to generate motor sequences instructed by visual cues (CUE condition), specifically LED lights indicating which lever to press next. The CUE condition was designed to probe scenarios in which sensory cues are processed based on learned rules and acted on in real-time, that is, it serves to model how many of our own motor sequences, such as following sheet music when playing an instrument, are assembled.

Beyond being overtrained on a single sequence or assembled on the fly in response to external cues, sequential behaviors can also be informed by recent events or actions, such as when we play or sing a recently heard tune. To probe the involvement of the MC in such WM-guided motor sequences, we also challenged animals to repeat a previously visually cued sequence from the WM condition (Fig. 1d; Methods and ref. 30). In contrast to the AUTO task, in which the progression of the prescribed motor sequence can be determined based on movement history alone, CUE and WM trials require external cues or internal WM-related processes to inform the serial selection of individual motor elements. The ‘flexible’ task (Fig. 1d) comprises both the CUE and WM conditions.

As reported previously³⁰, rats can learn to generate both cue-guided and WM-guided sequences. To probe whether MC is necessary for generating such flexible motor sequences, we lesioned it bilaterally (Extended Data Fig. 1; Methods) in animals that had reached expert performance on both the WM and CUE conditions (Methods and ref. 30).

Successful execution of the prescribed sequences was drastically reduced across both CUE and WM conditions (Fig. 3a,b), with postlesion success rates not significantly different from chance levels. We note that performance was also impaired after only lesioning MC in the hemisphere contralateral to the pressing limb (Extended Data Fig. 2; Methods). Lesioned rats also became more variable, or less systematic, in the errors they made (Fig. 3c). Although there was some improvement over the first 7 days postlesion, success rates and sequence variability did not recover to prelesion levels even after a month of additional training (Fig. 3a–c). One potential explanation for the postlesion drop in performance is that MC is required for the low-level control of the basic motor elements from which the flexible sequences are built. This, however, is unlikely as rats had no difficulty performing single lever presses in the CUE and WM task postlesion (Extended Data Fig. 3), consistent with previous findings^{5–7}. Thus, the most parsimonious explanation for our results is that MC contributes

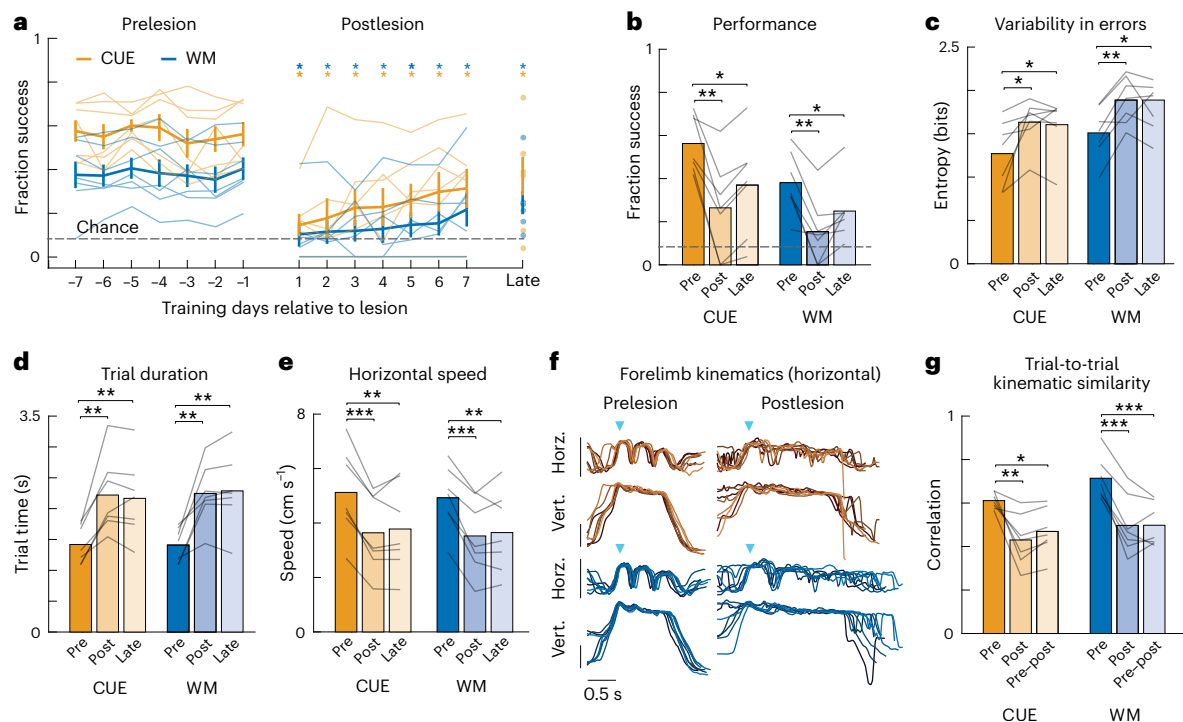


Fig. 3 | Flexible motor sequence execution depends on motor cortex.

a, Performance of cue-guided (CUE) and WM-guided motor sequences in the week before (prelesion), the week after (postlesion) and 1 month following (late) bilateral lesion. Shown is the fraction of successful trials, averaged over rats ($n = 7$; error bars are s.e.m.). Stars denote whether performance is significantly different on a given day, relative to average performance in the week before lesion, for each condition. Chance performance is defined as an 8.33% success rate, equivalent to guessing at the one in 12 sequences. Thin lines denote individual rats. **b**, Average performance over the week before (pre) and on days 3–7 after (post) MC lesion, and, to account for experience-dependent recovery, 1 month after lesion (late). Lines indicate individual rats ($n = 7$). Postlesion performance is not significantly different from chance levels ($P = 0.0725$ and $P = 0.2637$ for CUE and WM, respectively, one-sampled two-sided t test) **c**, Variability in the errors, as quantified through the Shannon entropy, for each

condition (CUE and WM) on 1,000 trials from before (pre), 3–7 days after (post) and 1 month after (late) lesion. Lines denote individual rats ($n = 7$). **d**, Duration (trial time) between the first and third lever presses for 1,000 trials before, 3–7 days after and 1 month after lesion. Lines indicate individual rats ($n = 7$). **e**, Same as **d** for trial speeds. **f**, Horizontal and vertical kinematic traces of the dominant forelimb for eight correct trials of the same sequence, overlaid, from one example rat. Shown are eight trials from the CUE (orange) and WM (blue) conditions, before and after the lesion. Blue arrows denote the time of the first lever press, and vertical bars indicate 100 pixels (Supplementary Videos 1 and 2) or approximately 3.5 cm. **g**, Trial-to-trial correlation averages for successful trajectories of the same sequence, time-warped to the lever presses, of the dominant forelimb (both horizontal and vertical components) of all rats ($n = 7$), before lesion, after lesion and across lesion conditions. * $P < 0.05$, ** $P < 0.01$ and *** $P < 0.001$, two-sided paired t test.

to the sequencing of subcortically generated motor elements when their serial order is informed by visual cues or WM.

That said, the detailed movement patterns associated with the sequences were altered following the lesions. Average trial times increased, and movement speeds were reduced (Fig. 3d,e). Forelimb movement trajectories also became more variable (Fig. 3f,g), even when performing the correct sequence. Interestingly, the postlesion movement patterns resembled what was seen early in learning (Extended Data Fig. 4), suggesting a reversion to species-typical movement patterns likely produced by motor circuits in the brainstem^{20,36}. Thus, in addition to having a role in specifying the sequential structure of the behavior, this indicates that the MC is also needed to generate the learned kinematics underlying effective transitions between individual elements, likely through actions on sensorimotor striatum^{8,30,37}. Intriguingly, the MC is only required to express such learned kinematics for flexible cue-guided sequences, not automatic ones (Fig. 2f versus Fig. 3g; $P = 0.015$ and $P = 0.0015$ for CUE and WM, respectively, two-sided t test), suggesting that its necessity in shaping and refining low-level kinematics is a function of the specific challenges associated with the task.

While these results suggest that MC is essential for both sequencing subcortically generated elements and for specifying task-specific learned kinematics, the inability to express the right sequence could, in theory at least, be due to confounding effects on low-level control.

After all, a clumsy and imprecise piano player may accidentally press the wrong key, making what is ostensibly a low-level control problem manifest as a deficit in high-level sequencing. However, unlike a piano, the ‘keys’ in our task are separated by physical barriers (Methods), requiring rats to make pronounced body movements toward the lever to be pressed (Extended Data Fig. 5a). Thus, incorrect presses due to imprecise forelimb or body control are unlikely. Consistent with MC having a role in cue-guided sequencing of movements, we found that the postlesion errors in the flexible task were predominantly due to orienting toward and pressing the ‘incorrect’ lever (Extended Data Fig. 5b; Methods).

Demands for flexibility interfere with the subcortical consolidation of automatic motor sequences

Thus far, we only considered scenarios in which a motor sequence is either overtrained to the point of automaticity (AUTO) or generated on the fly in response to instructive cues (CUE). In many cases, however, the motor elements that make up an automatic sequence are also reused in flexible contexts, such as the keypresses that constitute your password, which are used for typing other words³⁸. Note that in the flexible context, any of the motor elements making up the automatic behavior can be followed by a range of different movements or actions. This additional demand for flexibility could interfere with the subcortical consolidation of automatic sequences because subcortical circuits

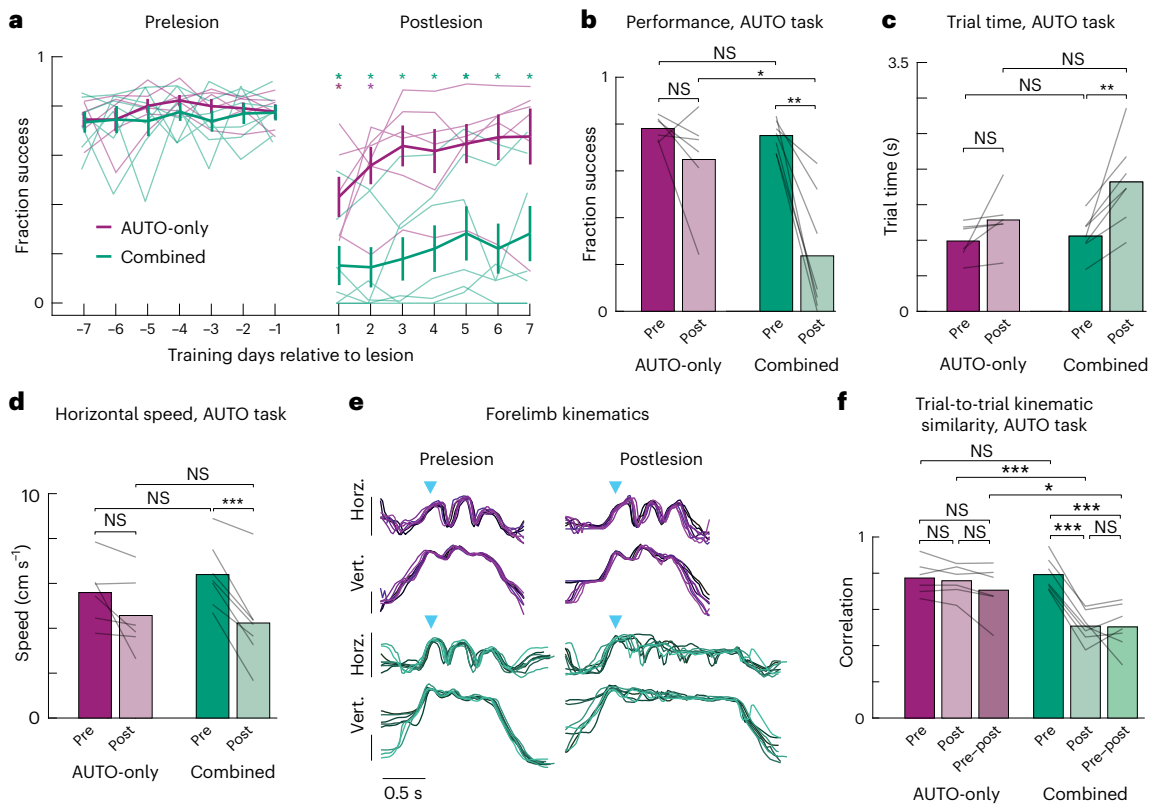


Fig. 4 | Interference across tasks renders automatic motor sequences motor cortex-dependent. **a**, Comparison of the performance in AUTO task sessions for rats trained on the combination of the automatic and flexible tasks ('combined'; $n = 7$, green lines, same cohort as Fig. 3) versus rats trained on the automatic task alone ('AUTO-only'; $n = 6$, purple, from Fig. 2a, error bars are s.e.m.), in the week before and after bilateral MC lesions. Stars denote whether performance is significantly different on a given day relative to average performance in the week before lesion for each cohort. Thin lines denote individual rats. Data from the AUTO-only cohort is replotted from Fig. 2. **b**, Average performance in the week before and 3–7 days following lesion in AUTO trials. Lines indicate individual rats. Postlesion 'combined' performance was not significantly better than

chance performance, defined as ($P = 0.1659$, one-sampled two-sided t test). **c**, Trial time plotted in the 1,000 trials before (pre) and after (post) lesion. **d**, As in **c** but for trial speed. **e**, Horizontal and vertical position of the dominant forelimb on eight example trials, sampled before and after the lesion, from one rat in each cohort (combined, green; AUTO-only, purple). Blue arrows denote the time of the first lever press, and vertical bars indicate 100 pixels or approximately 3.5 cm. **f**, Average trial-to-trial forelimb correlations (both horizontal and vertical positions), time-warped to the lever presses, of all rats before lesion, after lesion and across lesion conditions. * $P < 0.05$, ** $P < 0.01$ and *** $P < 0.001$, two-sided t test.

cannot unambiguously link the current motor element to the next one across different tasks.

To test whether automatic motor sequence execution becomes MC dependent when trained alongside flexible sequences assembled from similar movements, we lesioned MC in animals that had been overtrained on a single sequence while also performing the flexible task in separate experimental sessions (the 'combined' task; $n = 7$). In contrast to rats trained only on the automatic task (AUTO-only; $n = 6$; data from Fig. 2), rats in the combined task showed dramatically reduced performance on the automatic sequence following MC lesions (see Fig. 4a,b, Supplementary Video 3 and Supplementary Note for effect size comparison). Performance did not recover even after extended training (Extended Data Fig. 6). Movement kinematics were also disrupted (Fig. 4c–f) and accompanied by a significant increase in trial-to-trial variability (Fig. 4e,f).

The stark difference in the reliance on MC in the two training conditions could not be explained by prelesion training differences across the two cohorts or in the degree to which the overtrained sequence had become 'automatic' as per established definitions^{31,33,34}. Learning the overtrained task was not affected by the addition of the flexible task, with rats in both training cohorts reaching comparable success rates on AUTO task trials (Fig. 4b) in a similar number of training trials (Extended Data Fig. 7). They were also similarly engaged in terms of the numbers of trials per session and the number of training sessions

before lesion (Extended Data Fig. 7). Metrics describing the kinematics of the movement patterns were also similar before lesioning for the AUTO trials across the different training cohorts (Fig. 4c,d,f).

Overall, these results suggest that demands for the flexible reuse of motor elements that constitute an overtrained behavior prevent subcortical consolidation of the automatic sequence, rendering it MC-dependent.

A neural network model explains the mechanisms of subcortical consolidation and its interference

To pinpoint the circuit mechanisms and operational logic that give rise to the differential involvement of MC in automatic and flexible sequence execution and the interference effect we observe in the combined training condition, we developed a biologically inspired neural network model consisting of 'motor cortical' and 'subcortical' circuits (Fig. 5a). Given our previous finding that sensorimotor striatum (dorsolateral striatum (DLS) in rodents) is required for executing automatic sequences in this experimental paradigm³⁰, we refer to the subcortical region in the model as the 'DLS module'. However, we recognize that its contributions are made through actions on downstream brainstem controllers and likely also through thalamic loops^{20,25,39}.

We trained the model on a simulated version of our piano task, in which the model's output is tasked with moving a virtual manipulator in two dimensions sequentially to three distinct target regions

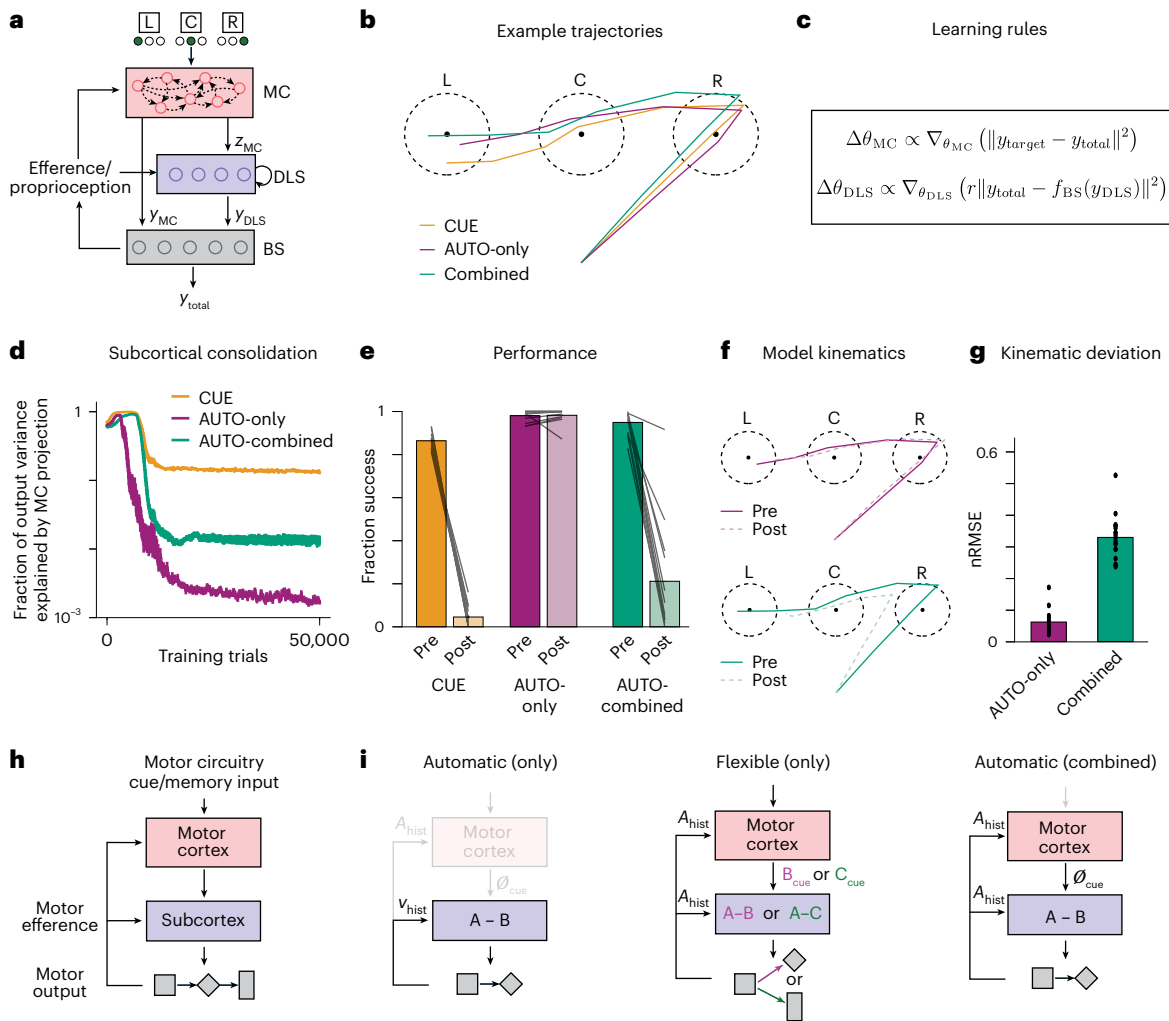


Fig. 5 | A neural network model reproduces the experimental results and predicts interference between automatic and flexible task conditions. **a**, Schematic representation illustrating the architecture of our neural network model. In this model, an MC module receives cue inputs and projects, via output z_{MC} to a downstream module that we equate with the DLS (see ‘A neural network model explains the mechanisms of subcortical consolidation and its interference’ for the rationale behind this interpretation). Both MC and DLS modules learn to interact with a BS control module via outputs y_{MC} and y_{DLS} to control the total motor output y_{total} . The BS module, in turn, sends efference/proprioceptive feedback to the MC and DLS modules. **b**, Example trajectories on a simulated version of the piano task following model training in either CUE, AUTO-only or AUTO-combined tasks. The network controls the velocity of a ‘forelimb’ and must move it into three circular regions (representing ‘lever presses’) in the correct sequential order (in this example, ‘right-center-left’ for all tasks). **c**, Learning rules for the MC and DLS modules (see ‘A neural network model explains the mechanisms of subcortical consolidation and its interference’ for details). y_{target} is the target trajectory for the current trial, used to train the MC module. This target signal is not intended to be biologically realistic but, rather, is an abstract way to capture the propensity of learning in MC to improve task performance; f_{BS} indicates the transformation applied by the brainstem module; θ refers to the weights of each module; and r indicates whether the trial was rewarded or not (that is, $r = 1$ for a correct trial and $r = 0$ for an incorrect trial). **d**, Measure of

engagement of the MC module throughout training for the CUE AUTO-only and AUTO-combined tasks, averaged over $n = 20$ training runs. **e**, Effects on task performance of ‘lesioning’ the MC module (that is, clamping its outputs z_{MC} and y_{MC} to zero). Lines indicate individual performance over $n = 20$ runs. **f**, Mean manipulandum trajectories, pre-MC and post-MC module removal, for the overtrained sequence ‘right-center-left’. **g**, Difference (normalized root mean squared error) between the average manipulandum trajectories before and after removing the MC module ($n = 20$ for each training condition). **h**, The motor circuit we consider for sequence production. **i**, Hypothetical roles for MC (red) and subcortex (blue) in generating discrete motor sequences. For a single automatic sequence (left), the mapping between past and future movements is unambiguous, meaning that motor efference/history is sufficient to specify the progression of the motor sequence, something that can be done subcortically. For flexible sequences (center), the transition between elements is inherently ambiguous and cannot be specified simply by mapping past to future actions (for example, action A can transition to either action B or C depending on the sequence). Thus, when challenged to produce an automatic sequence in the context of combined training on both tasks (right), concurrent demands for flexibility interfere with a rote mapping between past to future actions and hence prevent subcortical consolidation of the automatic motor sequence, making it dependent on inputs from MC.

(corresponding to the three levers in the in vivo version of the task; Fig. 5b). We modeled the DLS module as a recurrent network, with the recurrence corresponding to inhibitory connections among striatal projection neurons as well as loops through the thalamus and basal ganglia^{39–41}. The DLS module receives input from the MC module as well as efference/proprioceptive feedback about the current state

of the manipulandum from a brainstem/spinal cord (BS) module. These choices reflect the known anatomy of the corresponding motor circuits^{20,25,39,41}. Motivated by our previous finding showing that the activity of DLS neurons at lever-press times is minimally sensitive to lever identity³⁰, sensory cues instructing the sequence of ‘lever presses’ in the model were provided to the MC but not the DLS module.

The outputs of the MC and DLS modules are integrated by the BS module, which transforms them into motor commands to produce kinematics.

In our model, the MC module is trained using standard supervised machine-learning techniques (Methods) to ensure that the total output of the model—that is, the MC output combined with that of the subcortical pathway—produces the correct movement sequence (Methods; Fig. 5c). The DLS module, by contrast, is trained using reinforcement learning, a choice motivated by extensive literature supporting a model of dopamine-modulated reinforcement learning in dorsal striatum^{42–45} (Fig. 5c). Notably, the action being reinforced is the output of the whole system, which reflects the contributions of both the MC and DLS modules. This kind of learning rule, known in the machine-learning literature as an ‘off-policy’ reinforcement learning algorithm, incentivizes subcomponents of a larger system (here the DLS module vis à vis the entire model) to assume autonomous control of behavior when possible⁴⁶. Such an objective is a plausible mechanism for encouraging subcortical consolidation in the motor system and is supported by experimental evidence^{20,47–49}. Biologically, this learning rule requires an efference copy of the motor command to be provided to DLS^{50–52} and reward-triggered dopamine release that modulates striatal plasticity^{45,53}. The consistent coincident activity of both signals should then strengthen the striatal connections that map past to future actions, thus consolidating control over a movement sequence.

We constructed our modeling framework to distinguish automatic (AUTO-only) and cue-guided (CUE) motor sequence execution, as these capture the essential distinctions in our experimental data, setting aside for this analysis the WM-guided task. We first trained models only on either the AUTO or the CUE task. For the former, no cue input was provided to the system, and one particular sequence served as the target sequence for all trials. In the CUE task, the target sequence varied across trials, and cues—inputs indicating the position of the next ‘lever’ to be ‘pressed’—were provided to the MC module. Throughout the training, the MC module contributed an increasingly smaller fraction to the total output of the models trained on the AUTO-only task but not the models trained on the CUE task (Fig. 5d). After models reached asymptotic expert performance, we ‘lesioned’ the MC module by silencing its outputs to the DLS and brainstem modules. The models qualitatively reproduced the experimental lesion results, with models trained in the AUTO-only but not the CUE task, showing robustness to the lesion (Fig. 5e).

Our model proposes a mechanism for this disparity—to control the behavior in our task without MC, the DLS module must be able to produce the correct movement trajectory based on its subcortical inputs alone (that is, recurrent and efference/proprioceptive information). This is not possible in the CUE task when the behavior is flexible because subcortical circuits do not have information about the cue inputs that define the correct sequence. In the AUTO task, on the other hand, the sequence is fully specified by previous movement history, allowing successful subcortical consolidation following sufficient training. It is important to note that the model recapitulating our experimental results is a direct consequence of the reinforcement learning rule in the DLS module and of MC having privileged access to the instructive sensory cues, both biologically plausible model features^{16,42,43,53–55}.

Next, to probe whether this same model can account for the interference of subcortical consolidation observed in our experiments, we trained it simultaneously on both the AUTO and CUE tasks (‘combined’). By adding this demand for flexibility and the consequent ambiguity in sequence order across tasks, reinforcement learning in the DLS module could not proceed, as reward and motor efferent signals were no longer unambiguously linked. This prevented subcortical consolidation of the automatic sequence (Fig. 5d), leaving it dependent on the MC module for successful sequencing (Fig. 5e) and for producing the correct kinematics (Fig. 5f,g). Of note, interference across the tasks requires DLS

module activity to be similar for AUTO and CUE trials, which is known to be the case in our task³⁰.

Together, these results clarify the role of MC in sequencing movements and the conditions under which motor sequences can be consolidated subcortically (Fig. 5h,i).

Discussion

To address the role of MC in motor sequence execution, we trained rats to generate three-element lever-press sequences in two distinct task contexts—after a single sequence had been overtrained to the point of automaticity and when sequences were instructed by visual cues (Fig. 1). While we found MC to be dispensable for performing automatic motor sequences when trained in isolation (Fig. 2), it was required for flexible cue-guided sequences (Fig. 3). However, when the automatic sequence was practiced alongside flexible ones, it remained MC dependent (Fig. 4). A simple neural network model reproduced these findings and provided a circuit-level explanation for the experimental observations (Fig. 5).

That single motor sequences overtrained in our piano task survived MC lesions (Fig. 2) corroborates earlier results showing that stereotyped learned motor skills can be consolidated and executed subcortically^{6,26–28,56}. Previous studies implicating DLS in the storage and execution of such behaviors^{21,49,56,57} suggest that DLS transforms information about the animal’s current ‘state’ (for example, efference/proprioception) conveyed via thalamic inputs^{20,40,41} into a basal ganglia output that, through actions on downstream control circuits, specifies automatic learned behaviors. When simulating this circuit logic in a network model, we showed that subcortical specification and consolidation proceeded for rote stereotyped motor sequences that, once initiated, are fully specified by behavioral history.

Moving beyond stereotyped automatic behaviors, we probed motor sequences informed by visual cues and WM, where sequence progression is contingent on environmental cues. In contrast to a previously described role for MC in correcting or adjusting locomotion based on environmental cues^{9,14,18}, we tested how discrete actions are selected and arranged in response to learned cue associations. We found that such flexible sequences remained dependent on MC even after lengthy training (Fig. 3). These results support the hypothesis that MC funnels information from behaviorally relevant cortical computations—for example, instructions based on learned sensorimotor associations or WM processes—to subcortical motor circuits, making them integral to executing complex flexible behavior^{9,16,18,25,29}.

From an evolutionary perspective, this makes sense—rather than duplicating or reinventing the robust and effective control functions of subcortical systems, MC can provide an adaptive advantage by orchestrating downstream controllers based on information uniquely available to them. Studies showing preparatory or planning activity in MC unrelated to ongoing movement control^{16,19,58,59} are consistent with the idea that MC has a role in flexible decision-making and action selection.

The process of selecting actions based on environmental state has typically been associated with the basal ganglia⁶⁰. However, we previously showed that the MC-contingent visually guided sequences we probe can be performed without the sensorimotor or associative arms of the basal ganglia, although lesions to the sensorimotor striatum led to slower and more variable kinematics³⁰. Our results are thus more consistent with a model in which MC instructs the serial order of actions, a function that does not seem to require the basal ganglia. The basal ganglia, however, may add state-specific kinematic refinements to the selected movements^{21,61}, an inversion of the standard model of action selection and execution in these circuits^{2,22,29,35,60}. However, we cannot rule out that other parts of the striatum contribute to aspects of sequencing beyond state-specific kinematics, such as tracking task context or parsing cue information during learning^{42,62–64}.

While our results revealed a clear dissociation in MC’s essential contributions to automatic and flexible behaviors, we discovered

that it was essential for generating automatic motor sequences when trained alongside the flexible task (Fig. 4). We argue that this is because a basic premise of subcortical consolidation—that the transitions between elements in a sequence are unambiguous (that is, fixed)—is violated for automatic sequences in our combined task. Learning a single stereotyped motor sequence guarantees that element A is always followed by B (our automatic task), and, hence, the transition A→B can be ingrained in subcortical circuits by mapping efference (or proprioceptive information) associated with A to an output that generates B. But if A can be followed by both B and C depending on sensory cues (our flexible task), additional information is required to transition from A (Fig. 5). Extracting behaviorally relevant environmental state information (and keeping it in WM) likely involves cortical processing^{54,55,65}, and our results suggest that MC is an essential conduit for conveying this information to subcortical motor circuits. However, if subcortical circuits are contingent on inputs from MC in one task regime (flexible task), our experimental and modeling results suggest that they will remain dependent on MC for generating automatic behaviors involving the same elements and transitions. Consequently, our model predicts that interference will be avoided when learning multiple tasks involving distinct motor elements (for example, lever presses versus nose pokes).

Whether this task interference extends more generally remains to be understood, but recent studies testing mice on multiple cognitive tasks have shown that cortical involvement depends on the demands imposed by the task^{66–68}. For example, while much of the cortex was found to be dispensable for a simple navigation task, several cortical areas become essential for performing the very same task in mice previously trained on a more complex, cognitively demanding navigation task⁶⁶. This result is consistent with our findings and suggests that even simple, subcortically controllable skills can become cortex-dependent when trained alongside a more cognitively demanding task.

Interference across multiple tasks has also been observed in human skill learning, where interleaving practice (that is, high interference) results in worse initial performance but better long-term retention and skill generalization than practicing skills in blocks⁶⁹. Interestingly, this phenomenon, called ‘contextual interference’, has also been associated with differing demands on human MC^{70,71}, where skills learned under high interference rely on MC to a greater degree than skills that are not. Establishing a link between the contextual interference effect in humans and our interference result in rats will require further exploration.

That subcortical consolidation of an automatic motor sequence can proceed under some task conditions but not others may reflect a trade-off between competing goals of the motor system. On the one hand, it makes sense to consolidate often-used motor sequences subcortically, thus making them less susceptible to cognitive interference and freeing up the cortex for other computations^{38,47,72,73}. However, permanent changes to subcortical circuits, induced by overtraining a single motor sequence²⁰, could make it more difficult to modify or reuse basic motor elements in other contexts because these may have become associated with specific transitions and sequences. We note that similar tradeoffs between specialization and flexibility have been observed also in cognitive tasks⁷⁴.

One way to manage these tradeoffs and get around the interference across task domains would be for the same motor elements/transitions to have distinct neural representations in subcortical regions that implement learned state-action maps (presumably striatum) across the different behavioral contexts⁶². In other words, if the neural representation of state/action A in automatic task trials were distinct from the representation of A in flexible ones, the neural control system would treat the same motor elements and the transitions between them across the two tasks differently, thus preventing interference. The training regimes and experimental conditions under which interference across task domains can be avoided remain to be tested, but studies suggest

that strong contextual signals may help coax the system into avoiding interference across similar tasks and actions⁷⁵.

Online content

Any methods, additional references, Nature Portfolio reporting summaries, source data, extended data, supplementary information, acknowledgements, peer review information; details of author contributions and competing interests; and statements of data and code availability are available at <https://doi.org/10.1038/s41593-024-01792-3>.

References

- Brecht, M., Schneider, M., Sakmann, B. & Margrie, T. W. Whisker movements evoked by stimulation of single pyramidal cells in rat motor cortex. *Nature* **427**, 704–710 (2004).
- Evarts, E. V. Relation of pyramidal tract activity to force exerted during voluntary movement. *J. Neurophysiol.* **31**, 14–27 (1968).
- Ferrier, D. Experiments on the brain of monkeys.—No. I. *Proc. R. Soc. Lond.* **23**, 409–430 (1875).
- Neafsey, E. J. et al. The organization of the rat motor cortex: a microstimulation mapping study. *Brain Res. Rev.* **11**, 77–96 (1986).
- Darling, W. G., Pizzimenti, M. A. & Morecraft, R. J. Functional recovery following motor cortex lesions in non-human primates: experimental implications for human stroke patients. *J. Integr. Neurosci.* **10**, 353–384 (2011).
- Kawai, R. et al. Motor cortex is required for learning but not for executing a motor skill. *Neuron* **86**, 800–812 (2015).
- Kolb, B. Functions of the frontal cortex of the rat: a comparative review. *Brain Res.* **320**, 65–98 (1984).
- Lemke, S. M., Ramanathan, D. S., Guo, L., Won, S. J. & Ganguly, K. Emergent modular neural control drives coordinated motor actions. *Nat. Neurosci.* **22**, 1122–1131 (2019).
- Lopes, G. et al. A robust role for motor cortex. *Front. Neurosci.* **17**, 971980 (2023).
- Whishaw, I. Q., Pellis, S. M., Gorny, B. P. & Pellis, V. C. The impairments in reaching and the movements of compensation in rats with motor cortex lesions: an endpoint, videorecording, and movement notation analysis. *Behav. Brain Res.* **42**, 77–91 (1991).
- Passingham, R. E., Perry, V. H. & Wilkinson, F. The long-term effects of removal of sensorimotor cortex in infant and adult rhesus monkeys. *Brain* **106**, 675–705 (1983).
- Castro, A. J. The effects of cortical ablations on digital usage in the rat. *Brain Res.* **37**, 173–185 (1972).
- Lawrence, D. G. & Kuypers, H. G. The functional organization of the motor system in the monkey. I. The effects of bilateral pyramidal lesions. *Brain* **91**, 15–36 (1968).
- Drew, T., Jiang, W., Kably, B. & Lavoie, S. Role of the motor cortex in the control of visually triggered gait modifications. *Can. J. Physiol. Pharmacol.* **74**, 426–442 (1996).
- Akintunde, A. & Buxton, D. F. Origins and collateralization of corticospinal, corticopontine, corticorubral and corticostriatal tracts: a multiple retrograde fluorescent tracing study. *Brain Res.* **586**, 208–218 (1992).
- Ebbesen, C. L. et al. More than just a ‘motor’: recent surprises from the frontal cortex. *J. Neurosci.* **38**, 9402–9413 (2018).
- Ebbesen, C. L. & Brecht, M. Motor cortex—to act or not to act? *Nat. Rev. Neurosci.* **18**, 694–705 (2017).
- Heindorf, M., Arber, S. & Keller, G. B. Mouse motor cortex coordinates the behavioral response to unpredicted sensory feedback. *Neuron* **99**, 1040–1054 (2018).
- Li, N., Chen, T.-W., Guo, Z. V., Gerfen, C. R. & Svoboda, K. A motor cortex circuit for motor planning and movement. *Nature* **519**, 51–56 (2015).
- Wolff, S. B. E., Ko, R. & Ölveczky, B. P. Distinct roles for motor cortical and thalamic inputs to striatum during motor skill learning and execution. *Sci. Adv.* **8**, eabk0231 (2022).

21. Dhawale, A. K., Wolff, S. B. E., Ko, R. & Ölveczky, B. P. The basal ganglia control the detailed kinematics of learned motor skills. *Nat. Neurosci.* **24**, 1256–1269 (2021).
22. Ohbayashi, M. The roles of the cortical motor areas in sequential movements. *Front. Behav. Neurosci.* **15**, 97 (2021).
23. Lu, X. & Ashe, J. Anticipatory activity in primary motor cortex codes memorized movement sequences. *Neuron* **45**, 967–973 (2005).
24. Berridge, K. C. & Whishaw, I. Q. Cortex, striatum and cerebellum: control of serial order in a grooming sequence. *Exp. Brain Res.* **90**, 275–290 (1992).
25. Grillner, S. & Robertson, B. The basal ganglia downstream control of brainstem motor centres—an evolutionarily conserved strategy. *Curr. Opin. Neurobiol.* **33**, 47–52 (2015).
26. Hwang, E. J. et al. Disengagement of motor cortex from movement control during long-term learning. *Sci. Adv.* **5**, eaay0001 (2019).
27. Lashley, K. S. Studies of cerebral function in learning: V. The retention of motor habits after destruction of the so-called motor areas in primates. *Arch. Neurol. Psychiatry* **12**, 249 (1924).
28. Glees, P. & Cole, J. Recovery of skilled motor functions after small repeated lesions of motor cortex in macaque. *J. Neurophysiol.* **13**, 137–148 (1950).
29. Klaus, A., Alves da Silva, J. & Costa, R. M. What, if, and when to move: basal ganglia circuits and self-paced action initiation. *Annu. Rev. Neurosci.* **42**, 459–483 (2019).
30. Mizes, K. G. C., Lindsey, J., Escola, G. S. & Ölveczky, B. P. Dissociating the contributions of sensorimotor striatum to automatic and visually guided motor sequences. *Nat. Neurosci.* **26**, 1791–1804 (2023).
31. Abrahamse, E. L., Ruitenberg, M. F. L., de Kleine, E. & Verwey, W. B. Control of automated behavior: insights from the discrete sequence production task. *Front. Hum. Neurosci.* **7**, 82 (2013).
32. Krakauer, J. W., Hadjiosif, A. M., Xu, J., Wong, A. L. & Haith, A. M. Motor learning. *Compr. Physiol.* **9**, 613–663 (2019).
33. Hélie, S. & Cousineau, D. The cognitive neuroscience of automaticity: Behavioral and brain signatures. In *Advances in Cognitive and Behavioral Sciences* (ed. Sun, M.-K.) 141–159 (Nova Science Publishers, 2014).
34. Haith, A. M. & Krakauer, J. W. The multiple effects of practice: skill, habit and reduced cognitive load. *Curr. Opin. Behav. Sci.* **20**, 196–201 (2018).
35. Hikosaka, O. et al. Parallel neural networks for learning sequential procedures. *Trends Neurosci.* **22**, 464–471 (1999).
36. Ruder, L. & Arber, S. Brainstem circuits controlling action diversification. *Annu. Rev. Neurosci.* **42**, 485–504 (2019).
37. Pimentel-Farfan, A. K., Báez-Cordero, A. S., Peña-Rangel, T. M. & Rueda-Orozco, P. E. Cortico-striatal circuits for bilaterally coordinated movements. *Sci. Adv.* **8**, eabk2241 (2022).
38. Diedrichsen, J. & Kornysheva, K. Motor skill learning between selection and execution. *Trends Cogn. Sci.* **19**, 227–233 (2015).
39. Lanciego, J. L., Luquin, N. & Obeso, J. A. Functional neuroanatomy of the basal ganglia. *Cold Spring Harb. Perspect. Med.* **2**, a009621 (2012).
40. Mandelbaum, G. et al. Distinct cortical-thalamic-striatal circuits through the parafascicular nucleus. *Neuron* **102**, 636–652 (2019).
41. McElvain, L. E. et al. Specific populations of basal ganglia output neurons target distinct brain stem areas while collateralizing throughout the diencephalon. *Neuron* **109**, 1721–1738 (2021).
42. Cox, J. & Witten, I. B. Striatal circuits for reward learning and decision-making. *Nat. Rev. Neurosci.* **20**, 482–494 (2019).
43. Joel, D., Niv, Y. & Ruppin, E. Actor-critic models of the basal ganglia: new anatomical and computational perspectives. *Neural Netw.* **15**, 535–547 (2002).
44. Markowitz, J. E. et al. Spontaneous behaviour is structured by reinforcement without explicit reward. *Nature* **614**, 108–117 (2023).
45. Schultz, W., Dayan, P. & Montague, P. R. A neural substrate of prediction and reward. *Science* **275**, 1593–1599 (1997).
46. Lindsey, J. & Litwin-Kumar, A. Action-modulated midbrain dopamine activity arises from distributed control policies. *Advances in Neural Information Processing Systems* **35**, 5535–5548 (2022).
47. Kadmon Harpaz, N., Hardcastle, K. & Ölveczky, B. P. Learning-induced changes in the neural circuits underlying motor sequence execution. *Curr. Opin. Neurobiol.* **76**, 102624 (2022).
48. Pinsard, B. et al. Consolidation alters motor sequence-specific distributed representations. *eLife* **8**, e39324 (2019).
49. Miyachi, S., Hikosaka, O. & Lu, X. Differential activation of monkey striatal neurons in the early and late stages of procedural learning. *Exp. Brain Res.* **146**, 122–126 (2002).
50. Fee, M. S. The role of efference copy in striatal learning. *Curr. Opin. Neurobiol.* **25**, 194–200 (2014).
51. Melzer, S. et al. Distinct corticostriatal GABAergic neurons modulate striatal output neurons and motor activity. *Cell Rep.* **19**, 1045–1055 (2017).
52. Lindsey, J., Markowitz, J. E., Datta, S. R. & Litwin-Kumar, A. Dynamics of striatal action selection and reinforcement learning. Preprint at *bioRxiv* <https://doi.org/10.1101/2024.02.14.580408> (2024).
53. Calabresi, P., Picconi, B., Tozzi, A. & Di Filippo, M. Dopamine-mediated regulation of corticostriatal synaptic plasticity. *Trends Neurosci.* **30**, 211–219 (2007).
54. Hatsopoulos, N. G. & Suminski, A. J. Sensing with the motor cortex. *Neuron* **72**, 477–487 (2011).
55. Barthas, F. & Kwan, A. C. Secondary motor cortex: where ‘sensory’ meets ‘motor’ in the rodent frontal cortex. *Trends Neurosci.* **40**, 181–193 (2017).
56. Doyon, J. et al. Contributions of the basal ganglia and functionally related brain structures to motor learning. *Behav. Brain Res.* **199**, 61–75 (2009).
57. Rueda-Orozco, P. E. & Robbe, D. The striatum multiplexes contextual and kinematic information to constrain motor habits execution. *Nat. Neurosci.* **18**, 453–460 (2015).
58. Sul, J. H., Jo, S., Lee, D. & Jung, M. W. Role of rodent secondary motor cortex in value-based action selection. *Nat. Neurosci.* **14**, 1202–1208 (2011).
59. Murakami, M., Vicente, M. I., Costa, G. M. & Mainen, Z. F. Neural antecedents of self-initiated actions in secondary motor cortex. *Nat. Neurosci.* **17**, 1574–1582 (2014).
60. Mink, J. W. The basal ganglia: focused selection and inhibition of competing motor programs. *Prog. Neurobiol.* **50**, 381–425 (1996).
61. Dudman, J. T. & Krakauer, J. W. The basal ganglia: from motor commands to the control of vigor. *Curr. Opin. Neurobiol.* **37**, 158–166 (2016).
62. Hikosaka, O., Nakamura, K. & Nakahara, H. Basal ganglia orient eyes to reward. *J. Neurophysiol.* **95**, 567–584 (2006).
63. Brown, L. L., Schneider, J. S. & Lidsky, T. I. Sensory and cognitive functions of the basal ganglia. *Curr. Opin. Neurobiol.* **7**, 157–163 (1997).
64. Liljeholm, M. & O’Doherty, J. P. Contributions of the striatum to learning, motivation, and performance: an associative account. *Trends Cogn. Sci.* **16**, 467–475 (2012).
65. Guo, Z. V. et al. Flow of cortical activity underlying a tactile decision in mice. *Neuron* **81**, 179–194 (2014).
66. Arlt, C. et al. Cognitive experience alters cortical involvement in goal-directed navigation. *eLife* **11**, e76051 (2022).
67. Bolkan, S. S. et al. Opponent control of behavior by dorsomedial striatal pathways depends on task demands and internal state. *Nat. Neurosci.* **25**, 345–357 (2022).
68. Pinto, L. et al. Task-dependent changes in the large-scale dynamics and necessity of cortical regions. *Neuron* **104**, 810–824 (2019).

69. Magill, R. A. & Hall, K. G. A review of the contextual interference effect in motor skill acquisition. *Hum. Mov. Sci.* **9**, 241–289 (1990).
70. Janice Lin, C.-H. Brain–behavior correlates of optimizing learning through interleaved practice. *NeuroImage* **56**, 1758–1772 (2011).
71. Wright, D. et al. Consolidating behavioral and neurophysiologic findings to explain the influence of contextual interference during motor sequence learning. *Psychon. Bull. Rev.* **23**, 1–21 (2016).
72. Lindsey, J. & Litwin-Kumar, A. Selective consolidation of learning and memory via recall-gated plasticity. *eLife* **12**, RP90793 (2024).
73. Pashler, H. Dual-task interference in simple tasks: data and theory. *Psychol. Bull.* **116**, 220–244 (1994).
74. Yang, G. R., Cole, M. W. & Rajan, K. How to study the neural mechanisms of multiple tasks. *Curr. Opin. Behav. Sci.* **29**, 134–143 (2019).
75. Heald, J. B., Lengyel, M. & Wolpert, D. M. Contextual inference underlies the learning of sensorimotor repertoires. *Nature* **600**, 489–493 (2021).

Publisher's note Springer Nature remains neutral with regard to jurisdictional claims in published maps and institutional affiliations.

Springer Nature or its licensor (e.g. a society or other partner) holds exclusive rights to this article under a publishing agreement with the author(s) or other rightsholder(s); author self-archiving of the accepted manuscript version of this article is solely governed by the terms of such publishing agreement and applicable law.

© The Author(s), under exclusive licence to Springer Nature America, Inc. 2024

Methods

Animals

The care and experimental manipulations of all animals were reviewed and approved by the Harvard Institutional Animal Care and Use Committee. Experimental subjects were female Long Evans rats (strain code 006) 3 to 8 months at the start of training (Charles River, RRID: RGD_2308852).

Cohorts

Two separate cohorts of rats were used to test the effect of MC lesions. The first cohort ($n = 7$, 'combined') was trained on the combined cue-guided, WM-guided and automatic three-lever tasks. The second cohort ($n = 6$, 'AUTO-only') was trained only on the automatic task as described below.

Behavioral training

Water-deprived rats received four 40-min training sessions during their subjective night, spaced ~2 h apart. Starts of sessions were indicated by blinking house lights, a continuous 1 kHz pure tone and a few drops of water. At the end of each night, water was dispensed freely up to the daily minimum (5 ml per 100 g body weight).

Rats in the combined task cohort ($n = 7$) were trained in the three lever-press task or 'piano'-task as previously described³⁰. Briefly, water-restricted rats were initially trained on a single lever task, in which they were rewarded with water for pressing one of three levers (left, center or right) based on a visual cue (one of three LEDs positioned above each of the three levers). Rats reached learning criteria when they performed >90% successful single lever presses over 100 trials.

After reaching the criteria on the single lever task, rats transitioned (see ref. 30 for full details) to a three-lever task, in which they were rewarded with water for completing lever presses in a prescribed sequence. In three of the four nightly sessions ('flexible' sessions), the prescribed sequence was guided either by visual cues (CUE) or from WM by repeating the previous sequence. Sequences were presented in blocks of six trials, where the first, second and third trials were CUE, and the fourth, fifth and sixth trials were WM. Following the sixth trial, the prescribed three-lever sequence randomly changed. In the fourth nightly session (the 'automatic' session), a single three-lever sequence was overtrained to the point of automaticity (AUTO). The AUTO sequence was fixed for the duration of the experiment. Cues were initially provided but were removed throughout training.

For rats in the AUTO-only cohort ($n = 6$), all four nightly sessions were automatic sessions. AUTO-only rats were either trained using cues, by initially learning the single-lever task before transitioning to the full three-lever automatic sessions, or through a trial-and-error process. Rats trained by trial-and-error never received any visual cues and instead were first pretrained to press any one of the three levers in exchange for a water reward. After 500 lever presses, rats then had to press a sequence of any three nonrepeating levers (for example, no left→left) before receiving a water reward. After 500 rewarded three-lever trials, rewards were probabilistically withheld (starting at 20% and increasing by 1% for each 50 rewarded trials) if the executed sequence did not match a specific and randomly chosen three-lever sequence.

Performance and learning rates, including expert success rate, task engagement (that is, levers pressed per session), trial times and the number of trials to reach expert criteria, did not significantly differ between the AUTO-only rats trained with cues or trained via trial and error ($P > 0.05$, two-sided t test). In total, five rats were trained with cues, and five rats were trained by trial and error. Three rats were excluded from the AUTO-only cohort because lesion volumes were small (<5 mm³). One rat was excluded due to hardware errors in the training box that emerged after the MC lesion.

Animals were used for manipulations after reaching expert criteria, defined as when the success rate on AUTO trials was greater than

>72.5% (following criteria in refs. 57,76,77), and when trial times and success rates of CUE, WM and AUTO trials stabilized to within 0.5σ of final performance (following criteria in ref. 26). Criteria in the AUTO trials were consistent with the development of motor automaticity as previously described from observations in human and primate studies (for example, improved performance, decreased trial times and extensive practice)^{33,34,78–84}.

To dissociate sequence errors due to imprecisions in forelimb control from sequence errors due to errors in action selection, we designed our levers 1 inch apart, separated by acrylic barriers 0.25 inches thick, 2.3 inches tall, which extend 1 inch from the wall. This required rats to make pronounced body and forelimb movements toward the lever to be pressed (Extended Data Fig. 5).

Lesion surgeries

MC lesions were performed as previously described^{6,21}. A thin glass pipette connected to a microinjector (Nanoject III; Drummond) was lowered into the cortex and 4.5-nl increments of ibotenic acid (1% in 0.1 M NaOH; Abcam) to a total volume of 108 nl per injection site, at a speed of <0.1 $\mu\text{l min}^{-1}$. Three injection sites at two depths were used in total, at locations specified in ref. 6.

Bilateral MC lesions were performed in two stages. After reaching asymptotic performance, the first cortical lesion was performed contralateral to the forelimb used for the first lever press in the AUTO sequence. After lesion and recovery (7 days), animals returned to training for at least 14 days (for a total of 21 days minimum in between lesion surgeries).

Histology

At the end of the experiment, animals were killed (100 mg kg⁻¹ ketamine and 10 mg kg⁻¹ xylazine) and transcardially perfused with either 4% PFA or 2% paraformaldehyde (PFA, source) and 2.5% glutaraldehyde (GA, source) in 1× PBS.

Brains perfused in 4% PFA were sectioned into 80 μm slices using a vibratome (Leica), then mounted and stained with cresyl violet to reconstruct lesion size. Brains perfused in 2% PFA and 2.5% GA were not sliced but stained with osmium, as described in ref. 85, and embedded epoxy resin for microcomputed tomography (CT) scanning. A micro-CT scan (X-Tek HMS St 225; Nikon Metrology) was taken at 130 kV, 135 μA with a 0.1 mm copper filter and a molybdenum source. 3D volume stacks were reconstructed with VGStudio MAX.

Quantification of lesion size

To determine the extent and location of the cortical lesions in our scanned Nissl slides ($n = 2$, 48 slices analyzed in each), we manually marked lesion boundaries on each slice and estimated the total lesion volume. The remainder of our MC lesions ($n = 11$), which were stained with osmium and reconstructed into a 3D.tiff stack, were analyzed and quantified in Fiji. First, the brains were aligned along the coronal, medial and sagittal planes. Next, we estimated the location of each coronal stack from bregma using anatomical landmarks (corpus callosum split and anterior commissure split). Finally, we used an image intensity threshold to separate the lesion from the brain and then computed the volume of this region in mm³. To qualitatively view the lesion extent, we projected the 3D stack along the DV axis and outlined the boundaries of the lesion (Extended Data Fig. 1).

Behavioral metrics

Performance metrics were calculated as defined previously in ref. 30. They include success rate, trial time, trial speed, error variability and error modes, which are discussed below.

Success rate. Success rate was defined as the number of rewarded trials divided by the total number of attempted trials.

Trial time. Trial time was defined as the interval between the first and third lever presses. This only includes successful sequences, as incorrect sequences may not include three lever presses.

Trial speed. Trial speed was defined as the average horizontal speed the rat moves throughout the trial, calculated by dividing the total distance, in cm, horizontally traveled between levers 1–2 and levers 2–3 by the trial time.

Error variability. Error variability was defined as the Shannon entropy (in bits) of the probability of each sequence occurring for a given target sequence. Low probability sequences ($P < 0.001$) are discarded. If mistakes are systematic, the probability distributions will be skewed toward particular erroneous sequences, and the entropy will be low. If mistakes are made randomly, the distribution will look more uniform, and the entropy will be high. For CUE and WM sequences, the error calculation was done on the sequence chosen for the AUTO condition.

Error modes. Errors were classified as ‘motor’ or ‘sequence’ as defined previously in ref. 30. Briefly, we define ‘motor error’ as an error that occurs when the rat orients toward the ‘correct’ lever but fails to depress it beyond the detection threshold. Sequence errors, on the other hand, occur when rats orient toward an ‘incorrect’ lever and fully depress it. For each session type (flexible and automatic) and lesion condition (prelesion/postlesion), ~100 videos of error trials were manually inspected and labeled.

Kinematic tracking

To determine the movement trajectories of the forelimbs of the animals in our task, we used machine-learning methods that use neural networks to determine the position of body parts in individual video frames^{86,87}. Videos of animals performing the task were acquired at 40 Hz and saved in 10 s chunks throughout the session. We extracted ~250 frames randomly from videos throughout training, per rat, and manually labeled the position of the forelimbs in each frame. This dataset was used to train neural networks for each animal.

Tracking accuracy was validated post hoc by visually inspecting five trials (~200 frames each) from each rat across three different sessions. Frames with poor tracking (<0.95 score from the model), typically due to occlusion, were removed and linearly interpolated over. Any trial with >10% of frames that were poorly tracked was discarded from any analysis. The full trajectory was then smoothed using a Gaussian filter with a σ of 0.6 frames. To assess kinematic similarity qualitatively across trials, we randomly sampled eight trials from the rat’s median trial time across all contexts.

Spatial entropy (Extended Data Fig. 5b) was computed, in 2.5 pixel bins, from the position of the nose across 2,000 trials. The resulting histogram was smoothed with a 2D Gaussian filter with an s.d. of 5 pixels before computing the Shannon entropy.

Kinematic metrics

To quantitatively compute kinematic similarity for movements of varying trial times, we aligned each trial by local-linearly warping the trajectory to the median trial length, using the lever taps as anchor points. We then computed trial-to-trial correlations (Pearson’s) of the concatenated x and y forelimb positions. The grand average was taken over all different trial-to-trial correlations.

Trial selection for behavioral analyses

Behavioral metrics were assessed before and after the bilateral lesion. For the fraction of successful trials, we selected the 7 days before surgery and the 7 days after returning to the training box (14 days in total postsurgery, including 7 days for recovery), excluding the first 2 days postlesion to account for nonspecific effects of surgery. For trial time and horizontal speed, we selected the 1,000 trials before

and following the lesion. For trial-to-trial trajectory similarity, we select from within 200 trials before and following the lesion. For behavioral metrics assessed late after the lesion, we used 1,000 trials starting from 1 month following the bilateral lesion for fraction correct and trial times, and 200 trials starting from 1 month following the bilateral lesion to compute forelimb correlations. The sequence used in the trial-to-trial trajectory similarity is chosen to match the AUTO sequence performed.

Effect sizes for comparisons across cohorts were computed as the proportional difference in prelesion and postlesion performance.

Following bilateral lesion, the combined task cohort performed a range of 57–121 days ($8,837 \pm 1,436$ CUE, $4,726 \pm 1,352$ WM and $16,454 \pm 4,664$ AUTO trials), and the AUTO-only cohort performed 39–103 days ($37,015 \pm 6,433$ trials) before the experiments were ended. Though no specific criteria were used to determine the end of experiments, these training times approximate the time it took to initially learn and reach asymptotic performance on the three-lever task (83 ± 42 days for CUE ($9,806 \pm 2,534$ trials), 72 ± 40 days for WM ($4,261 \pm 2,171$ trials) and 124 ± 34 days for AUTO ($8,979 \pm 2,047$ trials)).

Neural network models

Following the modeling in ref. 30, we modeled a simplified version of the experimental task in which a neural network agent controls the velocity of a manipulandum (represented as a point) in two dimensions. The agent is tasked with moving the manipulandum into a set of three circular target zones in a prescribed sequential order, as in the experimental task. The target zones were positioned as shown in Fig. 5b. If the sequence was not performed successfully within $T = 10$ timesteps of the simulation, the trial was halted and considered a failure.

We simulated an artificial neural network consisting of two populations, one corresponding to MC (the ‘MC module’) and another to subcortical circuits including DLS (the ‘DLS module’). Both modules were modeled as recurrent networks with 500 units. Each module projects via a linear layer synaptic weights to a downstream population (the ‘brainstem module’) consisting of 50 units, which itself outputs two-dimensional velocity signals after a final linear transformation. All units in the model used rectified linear (ReLU) nonlinearities. Network weights were initialized with the Kaiming uniform initialization⁸⁸.

Both the MC module and DLS module receive motor efference input indicating the kinematics output at the previous timestep. Additionally, in the cued task condition, the MC module receives cue information in the form of a vector indicating the position of the currently cued target zone relative to the forelimb. Cue signals are provided upon trial initiation and following each successful ‘lever press’ and are transiently active for one time step only. Each network consists of 500 units with a ReLU activation function. In the automatic task condition, the cue vector is clamped at zero.

The parameters (input, recurrent and output weights) of the MC and DLS modules were trained as follows. At each time step, a target velocity was determined, defined as the vector between the agent’s current position and the current target, scaled by a gain factor of 0.5. MC parameters were trained using backpropagation to minimize the squared distance between the target velocity and the velocity output by the agent (that is, the output of the brainstem module, taking into account the DLS module contributions as well; Fig. 5c). DLS parameters were updated using backpropagation to minimize the squared distance between the velocity output by the agent and the velocity that would be output by DLS alone (by passing the output of the DLS module alone through the brainstem module), multiplied by the ultimate reward value on that trial (1 for success and 0 for failure; Fig. 5c). To encourage independence of DLS from MC inputs, an additional penalty was imposed on the strength of the MC–DLS projection activity. Thus, the DLS module used a reinforcement learning rule (with no access to the target velocity), whereas the MC module learned using an error-based supervised learning rule.

The entire network was trained alternately on cued and automatic task trials for 50,000 total trials. On cued trials, the target lever sequence was sampled randomly, with all 12 possible target sequences equally likely. On automatic trials, the target sequence was always clamped to the same sequence for a given simulation (across different simulations, the automatic sequence was sampled randomly). All network training used backpropagation and the Adam optimizer with a learning rate set to 3×10^{-6} . The training was conducted using PyTorch.

Statistical analysis

No statistical methods were used to predetermine sample sizes, but our sample sizes are similar to those reported in previous publications^{8,9,18,21,37}. Animals were excluded from experiments post hoc if the lesions were found to be outside the intended target area or affected additional brain structures ('lesion surgeries'). Data collection and analyses were not performed blind to the conditions of the experiments. Animals were randomly assigned to experimental groups.

The data distribution for these analyses was assumed to be normal, but this was not formally tested. All statistical tests were two-sided. The sample size, type of statistical test and *P* value range are indicated in figure legends. Exact *P* values are provided in the Supplementary Note.

Reporting summary

Further information on research design is available in the Nature Portfolio Reporting Summary linked to this article.

Data availability

The raw behavioral data and processed kinematic data used in this manuscript can be found online at <https://github.com/kmizes/MC-paper>. Raw kinematic data are available upon reasonable request. For databases/datasets used in tracking, see <https://pose.mpi-inf.mpg.de/#related>.

Code availability

The example code used in this manuscript is available online at <https://github.com/kmizes/MC-paper>. DeeperCut Implementation: <https://github.com/eldar/pose-tensorflow>.

References

76. Guo, J.-Z. et al. Cortex commands the performance of skilled movement. *eLife* **4**, e10774 (2015).
77. Thorn, C. A., Atallah, H., Howe, M. & Graybiel, A. M. Differential dynamics of activity changes in dorsolateral and dorsomedial striatal loops during learning. *Neuron* **66**, 781–795 (2010).
78. Ashby, F. G., Turner, B. O. & Horvitz, J. C. Cortical and basal ganglia contributions to habit learning and automaticity. *Trends Cogn. Sci.* **14**, 208–215 (2010).
79. Hardwick, R. M., Forrence, A. D., Krakauer, J. W. & Haith, A. M. Time-dependent competition between goal-directed and habitual response preparation. *Nat. Hum. Behav.* **3**, 1252–1262 (2019).
80. Wiestler, T. & Diedrichsen, J. Skill learning strengthens cortical representations of motor sequences. *eLife* **2**, e00801 (2013).
81. Wymbs, N. F. & Grafton, S. T. The human motor system supports sequence-specific representations over multiple training-dependent timescales. *Cereb. Cortex* **25**, 4213–4225 (2015).
82. Ramkumar, P. et al. Chunking as the result of an efficiency computation trade-off. *Nat. Commun.* **7**, 12176 (2016).

83. Wu, T., Kansaku, K. & Hallett, M. How self-initiated memorized movements become automatic: a functional MRI study. *J. Neurophysiol.* **91**, 1690–1698 (2004).
84. Matsuzaka, Y., Picard, N. & Strick, P. L. Skill representation in the primary motor cortex after long-term practice. *J. Neurophysiol.* **97**, 1819–1832 (2007).
85. Masis, J. et al. A micro-CT-based method for quantitative brain lesion characterization and electrode localization. *Sci. Rep.* **8**, 5184 (2018).
86. Leibe, B., Matas, J., Sebe, N. & Welling, M. (eds). *Computer Vision—ECCV 2016* 34–50 (Springer International Publishing, 2016).
87. Mathis, A. et al. DeepLabCut: markerless pose estimation of user-defined body parts with deep learning. *Nat. Neurosci.* **21**, 1281–1289 (2018).
88. He, K., Zhang, X., Ren, S. & Sun, J. Delving deep into rectifiers: surpassing human-level performance on imagenet classification. *Proceedings of the 2015 IEEE International Conference on Computer Vision (ICCV)* 1026–1034 (IEEE, 2015).

Acknowledgements

We thank K. Hardcastle, N. K. Harpaz, K. Laboy-Juarez, C. Bhatia, D. Aldarondo and P. Zmarz for discussions and comments on the manuscript. We also thank S. Luleu, M. Shah and G. Pho for technical support. We also thank S. Turney and the Harvard Center for Nanoscale Systems, for infrastructure and support. This work was supported by the National Institutes of Health (grants R01-NS099323-01 and R01-NS105349 to B.P.Ö.) J.L. was also supported by the DOE CSGF (DE-SC0020347). The funders had no role in study design, data collection and analysis, decision to publish or preparation of the manuscript.

Author contributions

K.G.C.M. and B.P.Ö. conceived and designed the study. K.G.C.M. conducted the experiments and analyzed the data. J.L. and G.S.E. designed and analyzed the model. K.G.C.M. and B.P.Ö. wrote the manuscript with input from J.L. and G.S.E.

Competing interests

The authors declare no competing interests.

Additional information

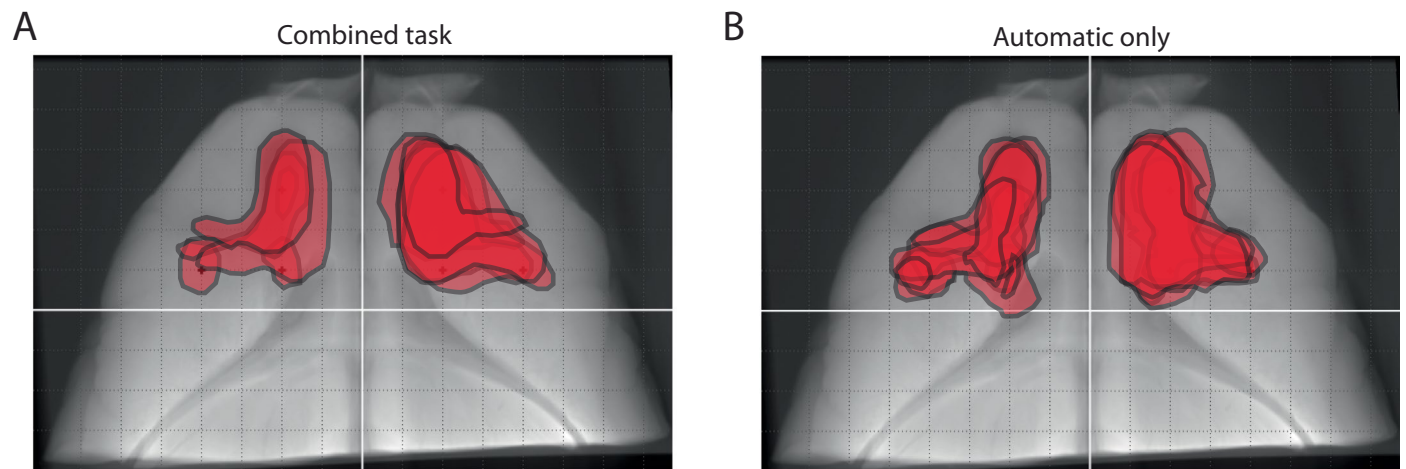
Extended data is available for this paper at <https://doi.org/10.1038/s41593-024-01792-3>.

Supplementary information The online version contains supplementary material available at <https://doi.org/10.1038/s41593-024-01792-3>.

Correspondence and requests for materials should be addressed to Kevin G. C. Mizes, G. Sean Escola or Bence P. Ölveczky.

Peer review information *Nature Neuroscience* thanks Jesse Goldberg, Pavel Rueda-Orozco and the other, anonymous, reviewer(s) for their contribution to the peer review of this work.

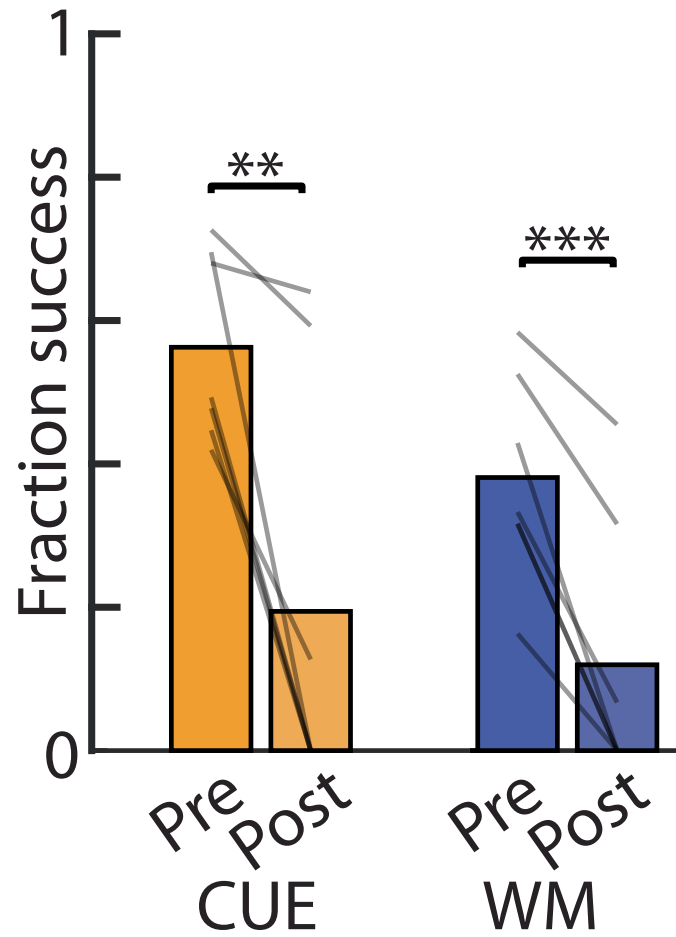
Reprints and permissions information is available at www.nature.com/reprints.

**Extended Data Fig. 1 | Histology from cohorts of MC lesioned rats.**

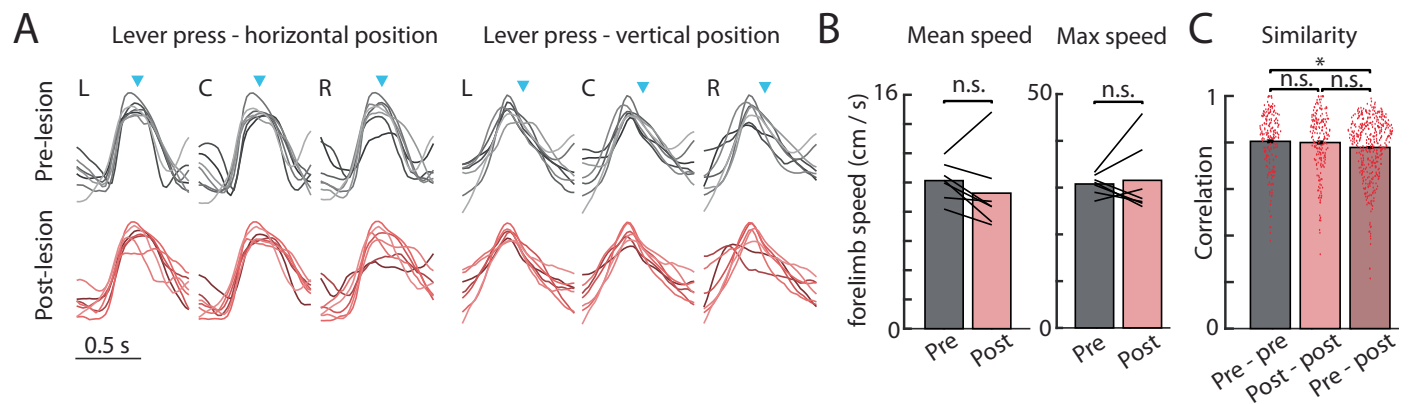
a,b, Outlines of MC lesion boundaries of rats imaged with micro-CT. White lines denote AP and ML from bregma, and dashed lines are spaced every 1 mm.

a, MC lesions of a cohort of rats trained on the combined task (CUE, WM and AUTO). Shown are outlines from $n = 5/7$ rats; two rats were imaged via Nissl stain.

b, MC lesions of a cohort of rats trained only on the automatic sessions ($n = 6$).

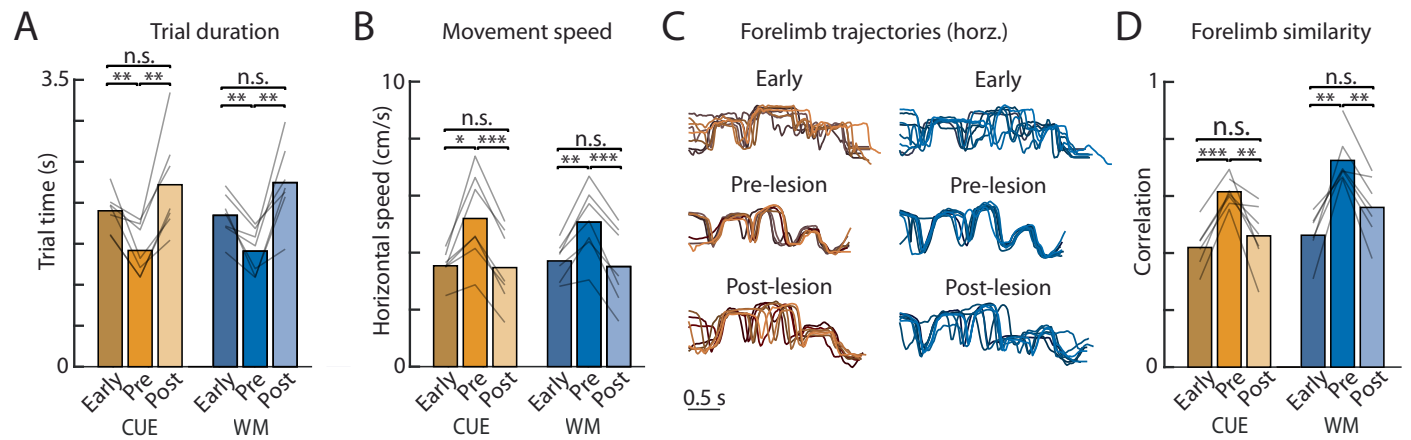


Extended Data Fig. 2 | CUE and WM performance following contralateral lesion. Fraction of successful trials pre- and post-unilateral lesion to the hemisphere contralateral to the lever-pressing forelimb, in the CUE and WM task. Lines denote individual rats ($n = 7$). $**P < 0.01$, $***P < 0.001$, two-tailed t-test.



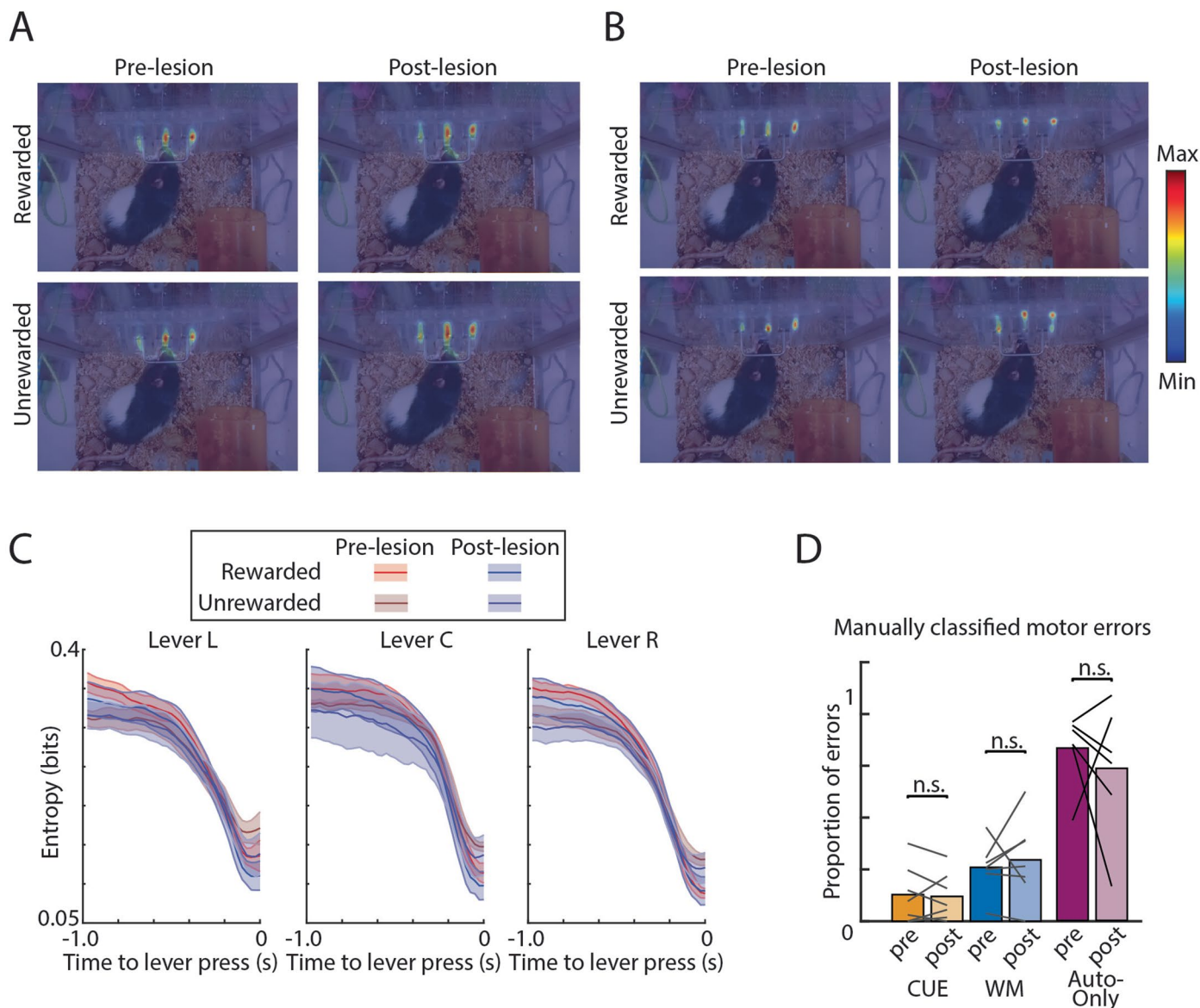
Extended Data Fig. 3 | Individual lever presses are species-typical and unaffected by the MC lesion. **a**, Average forelimb movement trajectories (scaled) for the left (L), center (C) and right (R) lever presses for all animals ($n = 7$) in the flexible task context. Each line denotes a different rat. Top row is the horizontal (left) and vertical (right) trajectories pre-lesion; bottom row is the trajectories post-lesion. **b**, Mean (left) and max (right) forelimb speed over single lever presses, before and after the lesion. Lines indicate individual rats

($n = 7$). $P > 0.05$, two-sided t-test. **c**, Correlation of the mean forelimb trajectory (horizontal and vertical) during a single lever-press, across levers (L, C or R) and rats ($n = 7$), giving us $n = 3 \times 7$ samples. Each dot indicates a correlation between individual samples. Comparisons are made across mean forelimb trajectories pre-lesion ($n = 210$), post-lesion ($n = 210$) and between pre-lesion and post-lesion trajectories ($n = 441$). For all subpanels, $*P < 0.05$, two-sided paired t-test. n.s. signifies $P > 0.05$.



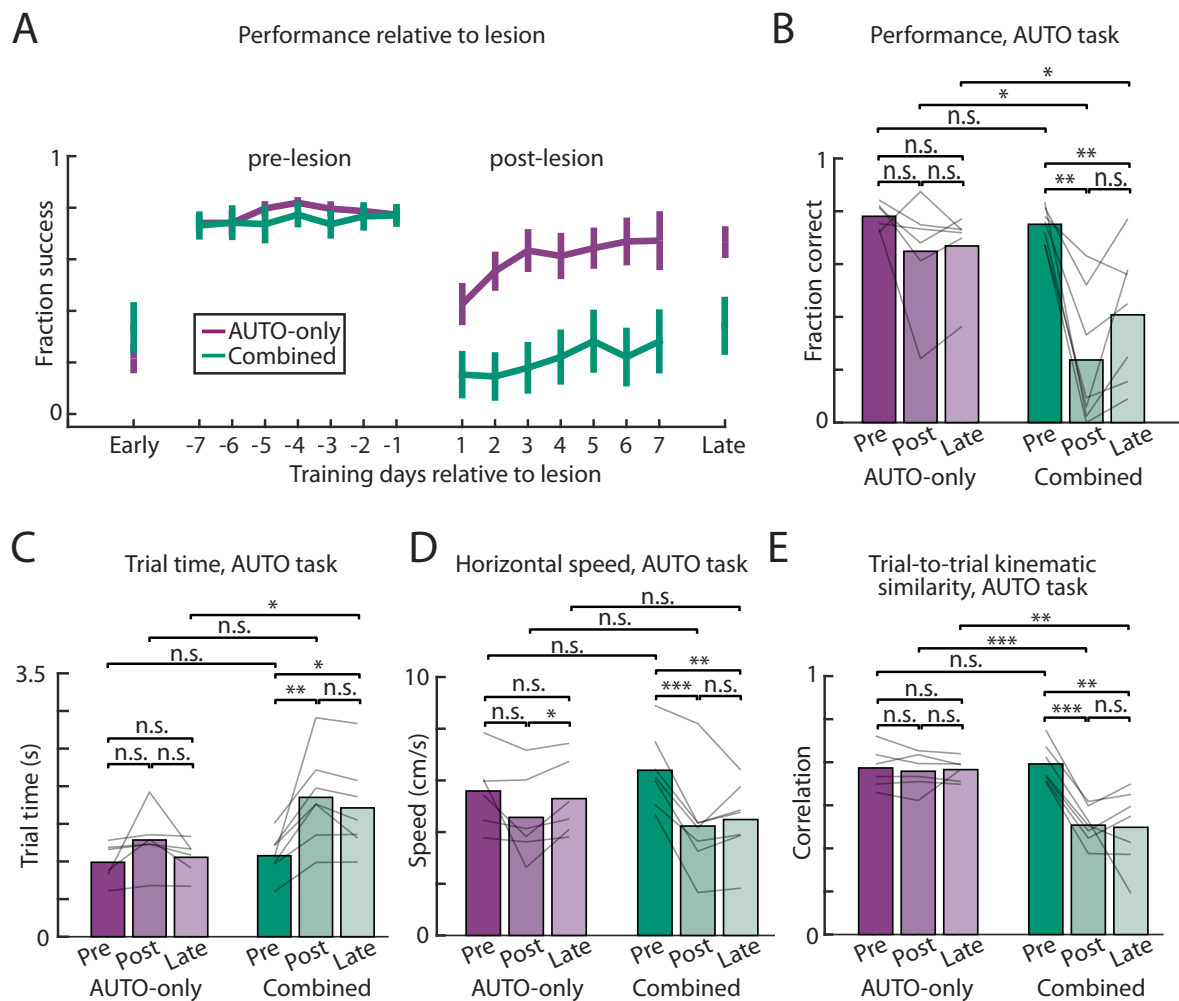
Extended Data Fig. 4 | Sensory- and working-memory-guided performance kinematics resembles performance early in training. a, b, Average performance ($n = 7$) over 1000 trials at the start of training, immediately pre-lesion and for the first training session post-bilateral lesion for (a) trial duration and (b) horizontal movement speed. c, Kinematic traces from one example rat early in learning

and before and after the lesion. d, Average trial-to-trial correlation of forelimb trajectories for a single sequence, averaged across all rats ($n = 7$). One of seven rats had no videos captured during early learning and was excluded from the 'early' analysis. * $P < 0.05$, ** $P < 0.01$, *** $P < 0.001$, two-sided paired t-test.



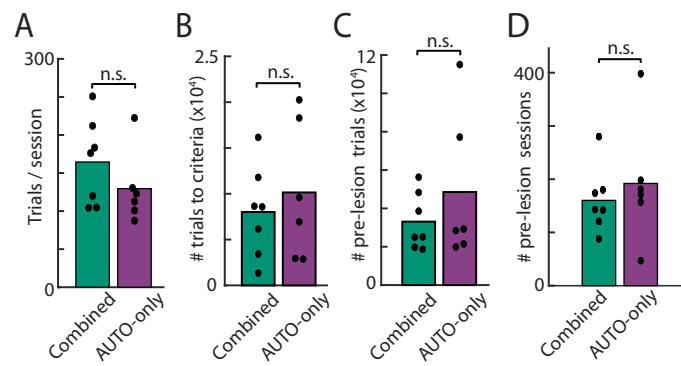
Extended Data Fig. 5 | Lever presses occur in discrete positions and error mode distributions. **a**, Spatial distributions of an example rat's nose for rewarded/unrewarded sequences, sampled pre- and post-lesion. **b**, Same as **a**, but the nose location is sampled only during the lever press. **c**, The variability of the nose position, quantified by computing the entropy of the spatial distribution across 2000 trials, for rewarded and unrewarded presses

(dark/light shades) and pre-lesion/post-lesion (red/blue), averaged across rats ($n = 5$). Two of the seven 'full task' rats did not have videos recorded from the top view and were excluded from this analysis. Shaded area indicates s.e.m. **d**, Proportion of error trials classified as 'motor errors' for both CUE and WM ($n = 7$), and the AUTO-only tasks ($n = 6$), across lesion conditions. $P > 0.05$, two-tailed t-test.



Extended Data Fig. 6 | Automatic task performance in combined cohort does not recover after one month of retraining. **a**, Performance in the AUTO task from the 1st week of training (early), 7 days before the lesion (pre-lesion), 7 days after the lesion (post-lesion) and 1 month following lesion (late) in the combined task (green, $n = 7$) and AUTO-only (purple, $n = 6$) cohorts. Error bars denote s.e.m. **b**, Average performance, measured as the fraction of successful trials, from time conditions (pre, post and late) across rats ($n = 6$ for AUTO-only and

$n = 7$ for combined cohorts), represented as individual lines. **c-e**, Kinematic metrics plotted in the week before lesion (pre), the week after lesion (post) and a month following lesion (late). **c**, Trial time. **d**, Trial speed. **e**, Forelimb trajectory correlation. Lines denote individual rats ($n = 6$ for AUTO-only and $n = 7$ for combined cohorts). * $P < 0.05$, ** $P < 0.01$, *** $P < 0.001$, two-sided paired (within cohort) or unpaired (across cohorts) t-test.



Extended Data Fig. 7 | Pre-lesion training metrics do not differ across the combined task and AUTO-only cohorts. **a**, Rats across both cohorts (combined task (n = 7) – green; and AUTO-only (n = 6) – purple) perform a similar number of trials per session before the MC lesion. Dots represent individual rat averages, and bars are grand averages. **b**, Both combined (n = 7) and AUTO-only (n = 6)

cohorts reach expert AUTO performance (Methods) in a similar number of training trials. **c, d**, Both cohorts (n = 7 for combined and n = 6 for AUTO-only) train for a similar number of total trials (**c**) and sessions (**d**) on the AUTO sequence before the lesion. $P > 0.05$ in all subpanels, two-sided unpaired t-test.

Reporting Summary

Nature Portfolio wishes to improve the reproducibility of the work that we publish. This form provides structure for consistency and transparency in reporting. For further information on Nature Portfolio policies, see our [Editorial Policies](#) and the [Editorial Policy Checklist](#).

Statistics

For all statistical analyses, confirm that the following items are present in the figure legend, table legend, main text, or Methods section.

n/a | Confirmed

- The exact sample size (n) for each experimental group/condition, given as a discrete number and unit of measurement
- A statement on whether measurements were taken from distinct samples or whether the same sample was measured repeatedly
- The statistical test(s) used AND whether they are one- or two-sided
Only common tests should be described solely by name; describe more complex techniques in the Methods section.
- A description of all covariates tested
- A description of any assumptions or corrections, such as tests of normality and adjustment for multiple comparisons
- A full description of the statistical parameters including central tendency (e.g. means) or other basic estimates (e.g. regression coefficient) AND variation (e.g. standard deviation) or associated estimates of uncertainty (e.g. confidence intervals)
- For null hypothesis testing, the test statistic (e.g. F , t , r) with confidence intervals, effect sizes, degrees of freedom and P value noted
Give P values as exact values whenever suitable.
- For Bayesian analysis, information on the choice of priors and Markov chain Monte Carlo settings
- For hierarchical and complex designs, identification of the appropriate level for tests and full reporting of outcomes
- Estimates of effect sizes (e.g. Cohen's d , Pearson's r), indicating how they were calculated

Our web collection on [statistics for biologists](#) contains articles on many of the points above.

Software and code

Policy information about [availability of computer code](#)

Data collection

Behavioral data was acquired using custom software, based on a design in Poddar et al. 2013, and implemented with Raspberry Pi 3 and Teensy 3.6 microcontrollers.

Data analysis

Data analysis was performed using custom code written in Matlab 2021b (Mathworks). Code is available at <https://github.com/kmizes/MC-paper>. For kinematic tracking, the DeeperCut 1.0 implementation in tensor-flow (Insafutdinov et al. 2016) was used (<https://github.com/eldar/pose-tensorflow>), together with custom code written in Matlab 2021b. Models were built and run using Pytorch version 1.12.1 in Python version 3.7.3.

For manuscripts utilizing custom algorithms or software that are central to the research but not yet described in published literature, software must be made available to editors and reviewers. We strongly encourage code deposition in a community repository (e.g. GitHub). See the Nature Portfolio [guidelines for submitting code & software](#) for further information.

Data

Policy information about [availability of data](#)

All manuscripts must include a [data availability statement](#). This statement should provide the following information, where applicable:

- Accession codes, unique identifiers, or web links for publicly available datasets
- A description of any restrictions on data availability
- For clinical datasets or third party data, please ensure that the statement adheres to our [policy](#)

The generated datasets are available at <https://github.com/kmizes/MC-paper>. Details and download of data used to pretrain DeeperCut can be found at: <https://pose.mpi-inf.mpg.de/>

Research involving human participants, their data, or biological material

Policy information about studies with [human participants or human data](#). See also policy information about [sex, gender \(identity/presentation\), and sexual orientation](#) and [race, ethnicity and racism](#).

Reporting on sex and gender	N/A
Reporting on race, ethnicity, or other socially relevant groupings	N/A
Population characteristics	N/A
Recruitment	N/A
Ethics oversight	N/A

Note that full information on the approval of the study protocol must also be provided in the manuscript.

Field-specific reporting

Please select the one below that is the best fit for your research. If you are not sure, read the appropriate sections before making your selection.

Life sciences Behavioural & social sciences Ecological, evolutionary & environmental sciences

For a reference copy of the document with all sections, see [nature.com/documents/nr-reporting-summary-flat.pdf](https://www.nature.com/documents/nr-reporting-summary-flat.pdf)

Life sciences study design

All studies must disclose on these points even when the disclosure is negative.

Sample size	No statistical methods were used to pre-determine the number of subjects in our study, but our sample sizes are similar to those reported in previous publications (Lemke et al., 2019, Dhawale and Wolff et al., 2021, Heindorf et al., 2018).
Data exclusions	Animals were excluded from experiments post-hoc if the lesions were found to be small or outside of the intended target area (n=3 animals were excluded based on these criteria).
Replication	All lesions were performed in multiple animals per group (n>=6) and yielded consistent, reproducible findings within each cohort.
Randomization	Animals were randomly assigned to experimental groups.
Blinding	Experimenters were not blinded to group allocation due to the nature of the experiment, as all animals needed to be prepared and handled individually, and K.G.C.M. performed all experiments alone.

Reporting for specific materials, systems and methods

We require information from authors about some types of materials, experimental systems and methods used in many studies. Here, indicate whether each material, system or method listed is relevant to your study. If you are not sure if a list item applies to your research, read the appropriate section before selecting a response.

Materials & experimental systems

n/a	Involvement
<input checked="" type="checkbox"/>	<input type="checkbox"/> Antibodies
<input checked="" type="checkbox"/>	<input type="checkbox"/> Eukaryotic cell lines
<input checked="" type="checkbox"/>	<input type="checkbox"/> Palaeontology and archaeology
<input type="checkbox"/>	<input checked="" type="checkbox"/> Animals and other organisms
<input checked="" type="checkbox"/>	<input type="checkbox"/> Clinical data
<input checked="" type="checkbox"/>	<input type="checkbox"/> Dual use research of concern
<input checked="" type="checkbox"/>	<input type="checkbox"/> Plants

Methods

n/a	Involvement
<input checked="" type="checkbox"/>	<input type="checkbox"/> ChIP-seq
<input checked="" type="checkbox"/>	<input type="checkbox"/> Flow cytometry
<input checked="" type="checkbox"/>	<input type="checkbox"/> MRI-based neuroimaging

Animals and other research organisms

Policy information about [studies involving animals](#); [ARRIVE guidelines](#) recommended for reporting animal research, and [Sex and Gender in Research](#)

Laboratory animals	Experimental subjects were female Long Evans rats (RRID: RGD_2308852) 3-10 months old at the start of training
Wild animals	The study did not involve wild animals.
Reporting on sex	Only female Long Evans rats were used in this study.
Field-collected samples	The study did not contain samples collected from the field.
Ethics oversight	The care and experimental manipulation of all animals were reviewed and approved by the Harvard Institutional Animal Care and Use Committee

Note that full information on the approval of the study protocol must also be provided in the manuscript.

Plants

Seed stocks	N/A
Novel plant genotypes	N/A
Authentication	N/A